International Journal of Environmental Sciences
ISSN: 2229-7359
Vol. 11 No. 8, 2025
https://theaspd.com/index.php

Solar Air Heating System With Coating And Rib Roughness On Absorber Plate: A Review

Firoz Alam[a]*, Madhava Nand Pandey[a]
[a]Department of Mechanical Engineering, National Institute of Technology Patna, India
*f.alam1.macet@gmail.com,

Abstract:
All processes in life are fuelled by energy, which is a fundamental source of power. Large amounts of energy are needed to keep the industrial revolution running. The majority of the world's energy needs are being satisfied by non-renewable and restricted conventional energy sources. Conventional sources of energy, in addition to their incapacity to supply our ever-increasing energy needs, are environmentally unsustainable. This is done to examine the performance based on various mass flow rate of air and sun intensity. The varied percentages of nanomaterial (0.1%, 0.2%, & 0.3%) are doped in black paint which increases the absorption of heat. The Reynolds number is changed for the fixed selective coating on absorber plate and mass flow rate. In addition, the impacts of entropy generation are explored with respect to solar radiation and ambient temperature. Thermophysical properties of nanofluids drastically altered due to size dependence of these properties. The heat transmission and thermal efficiency of a solar air heater with a V-shaped rib were evaluated statistically. Using a solar air heater with artificial roughness in the form of 30o incline ribs, thermal efficiency has been evaluated. On the upper side of the absorber surface, 15 mm and 20 mm pitches of inclined ribs were employed to create. The rib pitch values of 20 mm, and heat transmission statistics were studied for the comparison. Various geometrical aspects of the solar duct were mathematically calculated with an eye toward increasing the maximum heat transfer rate.
Keywords: *Nanomaterial, coating, Air temperature, Black Paint, sun intensity, Energy, Exergy.*

INTRODUCTION:

When using a passive solar air heating system, hot air is created at various sites and then directed to the final destination for use. The use of heat storing materials is popular in active SAH to create hot air during the off-peak hours. Passive SAHs, on the other hand, are typically utilized throughout the day. Single-pass and double-pass SAHs can be classed based on the number of air channels, with or without heat storage. There is just one channel for the air in a single-pass solar heater, and it flows either above or below the absorber plate, as shown in Figure 1.1. Figure 1.2 displays a double-pass solar heater, wherein air flows in two independent passageways, which can either be parallel or counter-clockwise. SAHs are typically constructed composed of an air duct and an absorber plate for absorbing sound. Thermal insulation with a low thermal conductivity is used to decrease heat losses from the bottom and sides. Many scientists have created their own experimental test rigs to study the consequences of adjustments made to the SAH's key components. As a result, the fundamental purpose of this research is to find the breadth of SAHs and investigate the various design configurations.

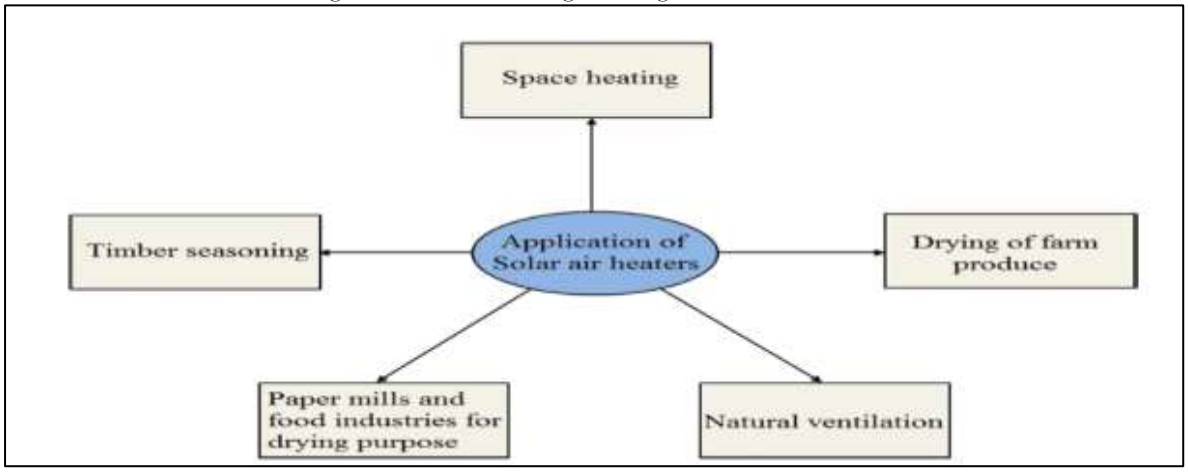

Figure 2. 1: Applications of solar air heater[1], [2]

International Journal of Environmental Sciences
ISSN: 2229-7359
Vol. 11 No. 8, 2025
https://theaspd.com/index.php

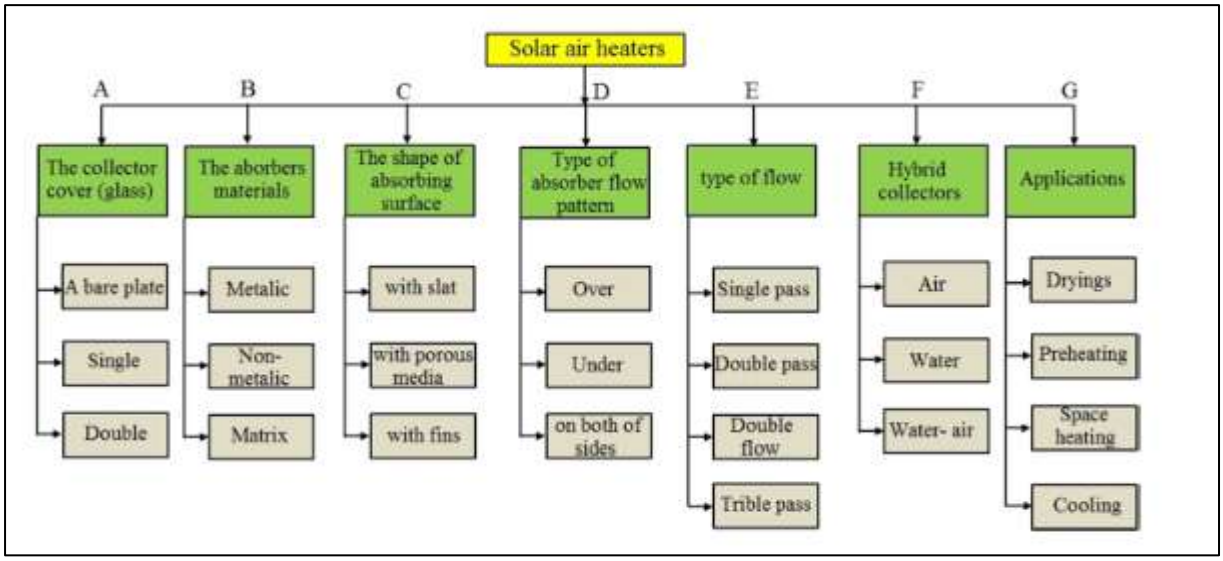

Figure 2. 2: Classification of solar air heater[3]

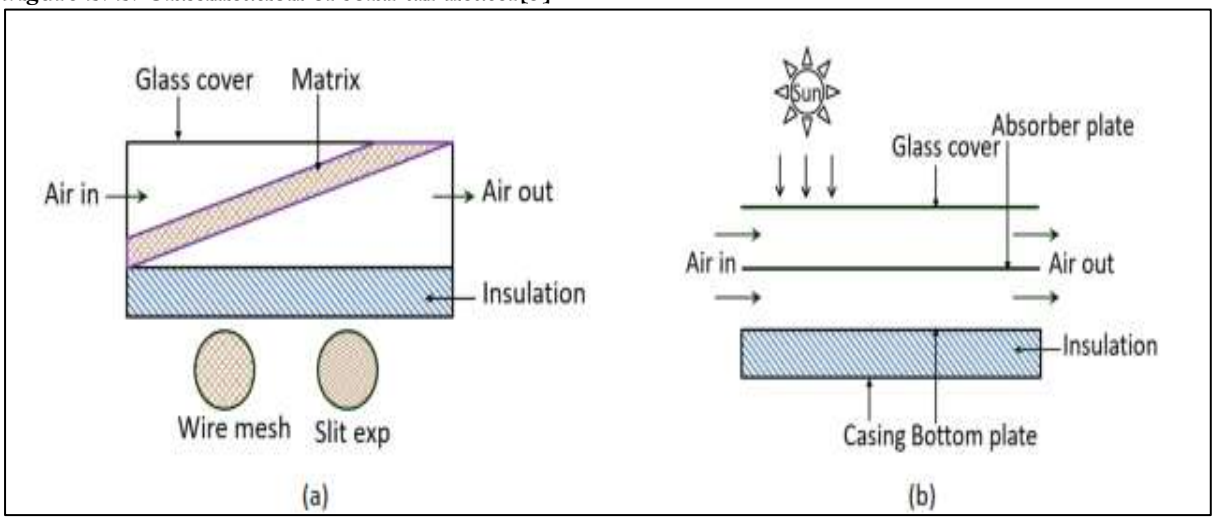

Figure 2. 3: Modification in solar air heater[4]

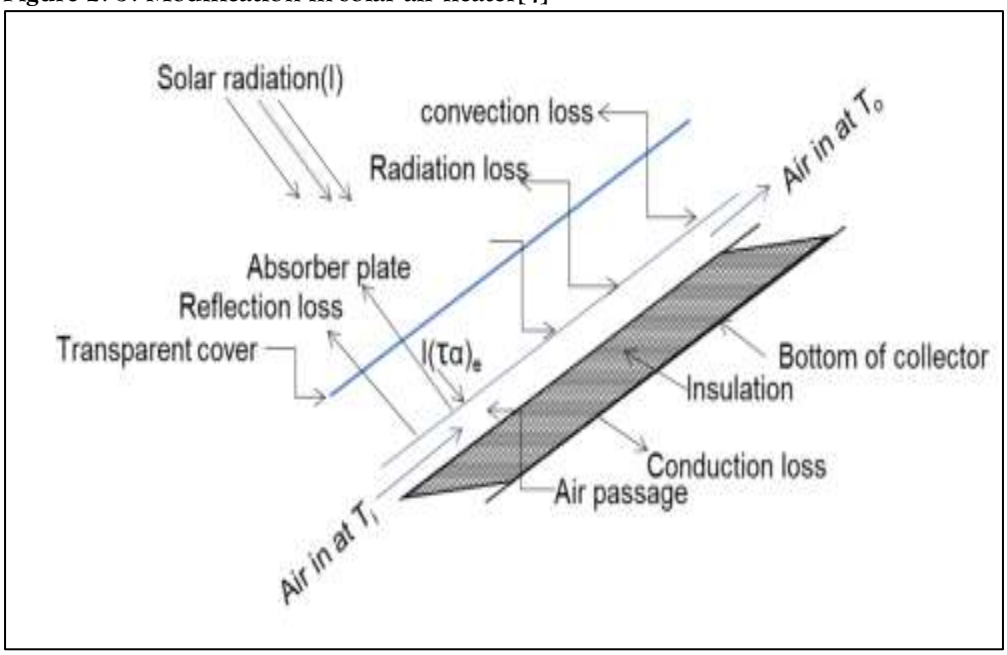

Figure 2. 4: Conventional solar air heater component[5][6]

2.1General Introduction

Researchers examined solar air heaters with artificial roughness added in the form of small diameter wires, machining ribs of various shapes, and generating dimple/protrusion in order to analyze the absorber plate's heat transmission increase rate. Studies on the use of artificial roughness in solar air heaters involve a wide range of forms to explore heat transfer and friction properties. When it comes to corrosion, boiling, freezing, and leaking, solar air heaters have a number of benefits over liquid warmers. Drying agricultural commodities with a solar air heater without thermal storage is a widespread approach. In practice, low-temperature drying of agricultural items (50–600 C) is frequent, and flat plate type solar air heaters make this practicable. Natural convection or induced convection are also possibilities for dispersing more hot air generated by an air heater.

Yadav et. al.[7] It was noticed that a solar air heater with roughened absorber surface wires was roughly 8 to 10 percent more efficient than a solar air heater with smooth wires when compared to another solar air heater with smooth wires. An investigation indicated that roughened solar air heaters are not beneficial for thermo hydraulic efficiency when the Reynolds number is more than 29000.

Wang et. al.[8] In order to increase the performance of the solar air collector, S-shaped ribs with gaps were added on the absorber surface. Under controlled testing settings, it was able to achieve an increase in thermal efficiency of between 13 and 48 percent.

Anil et. al.[9] created a relationship between the Nusselt number and the absorber surface, as well as generated gaps on the ribs of multiple V-shaped artificial roughness on the absorber surface. It was determined that the value of the Nusselt number grew by 6.74 times while employing this arrangement, but the friction factor also increased by 6.37 times in contrast to when it was utilized with a smooth surface.

Patel et. al.[10] The influence of NACA 0040 profile ribs organized in reverse sequence as a roughness element in a solar air heater was evaluated, and the results of the experiment showed that the thermo hydraulic performance was 2.53 at a Reynolds number of 6000, which is an increased performance.

Poongavanam et. al.[11] studies indicated that employing absorber surfaces with shot-blasted V-corrugations increased heat transmission on solar air heaters, and the Nusselt number obtained was higher than that of conventional solar air heaters while the friction factor was somewhat higher.

Anup kumar et. al.[12] Statistical study of a solar air heater's absorber surface was applied for numerical examination. Relative pitch roughness of 8, rib orientation angle of 60o, and twist ratio of 3 were selected to offer the maximum gain in thermal and exergetic efficiency over a smooth surface.

Sahu et. al.[13] This study compared the exergy efficiency of a solar air heater with one with an arc-shaped wire roughened absorber surface with that of a similar solar air heater with an absorber surface that was smooth, and it found the rough absorber surface to be 56 percent more efficient.

Singh et al[14] explored SAH utilizing two distinct roughness surfaces, one with many broken transverse ribs and the other with square wave shaped ribs, for both CFD and experimental reasons. For square-shaped rib roughened absorber surfaces, the maximum thermal hydraulic efficiency was more than double that of a plane absorber surface, but the pumping power needed was three times that of the plane absorber surface. There was a threefold increase in pumping power and absorber surface efficiency while treating SAH patients with several fractured ribs. For this test, researchers used ribs with a pitch to height ratio of 10 and a height to diameter ratio of 0.043.

Gawande et al.[15] A reverse L-shaped ribbed absorber surface was employed to assess the SAH's performance. These measurements were made at a relative roughness pitch of seven, a Reynolds number of 3800 to 18000, and at a constant relative roughness height of 0.042. The thermohydraulic performance of 1.90 was attained at a high heat transfer rate. R. Kumar et al [16] This triangle solar heater was tested utilizing graphene nonmaterial implanted in black paint to evaluate how efficient it was in generating heat. At a speed of 1 m/s, the system's maximum efficiency is 48.23%.

Manjunath et al[17] created turbulent air flow across the absorber surface by applying spherical rib roughness. A variety of Reynolds numbers was gathered, ranging from 4000 to 25000. There were spherical ribs ranging from 5 to 25 millimeters in diameter. In comparison to the baseline model, the Nusselt number was found to be two times larger. Scientists arrived to the conclusion that the greater thermal hydraulic performance offered by disc-shaped ribs.

International Journal of Environmental Sciences
ISSN: 2229-7359
Vol. 11 No. 8, 2025
https://theaspd.com/index.php

2.2Different Roughness Geometries Used in Solar Air Heater:

Researchers studied solar air heaters with artificial roughness added in the form of tiny diameter wires, machining ribs of various shapes, and generating dimple/protrusion in order to analyse the absorber plate's heat transfer increase rate. Studies on the use of artificial roughness in solar air heaters encompass a wide range of shapes to examine heat transmission and friction properties. When it comes to corrosion, boiling, freezing, and leakage, solar air heaters have a number of benefits over liquid heaters. Drying agricultural goods with a solar air heater without thermal storage is a common practice. In reality, low-temperature drying of agricultural products (50–60^0 C) is common, and flat plate type solar air heaters make this possible. Natural convection or forced convection are both options for delivering more hot air generated by an air heater. The type of fabrication and the environment are also factors to consider[18]–[20].

Table 2. 1: Different type of rib roughness

Ref.	Different rib roughness	Type
[6]	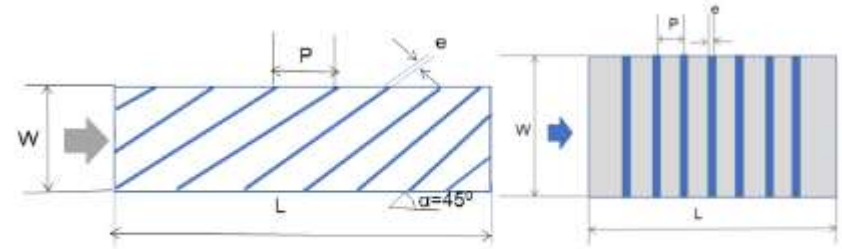	Straight
[6]	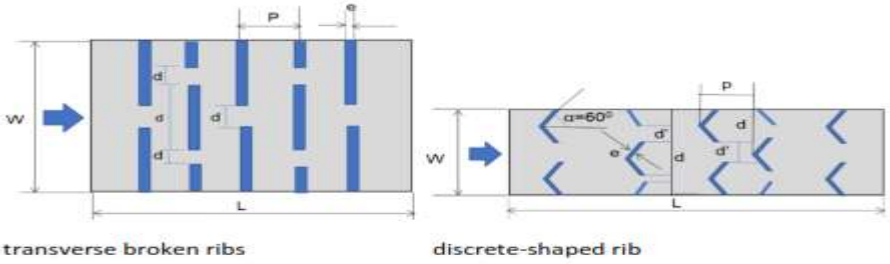	V shaped
[21]	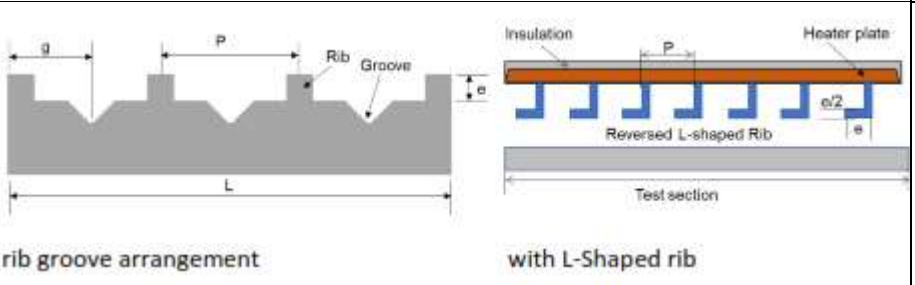	L shaped
[22][23]	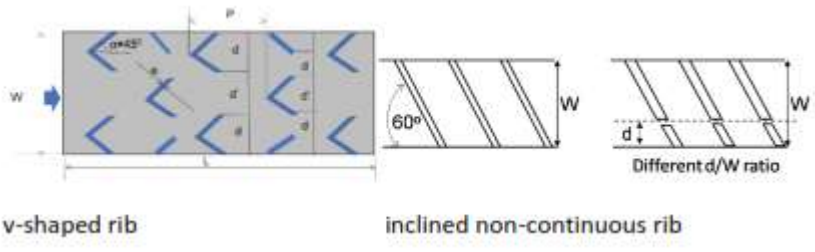	V shaped

[24][25]	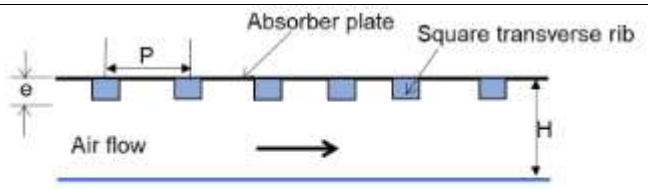 Square transverse ribs solar absorber plate	Rectangle
[26], [27]	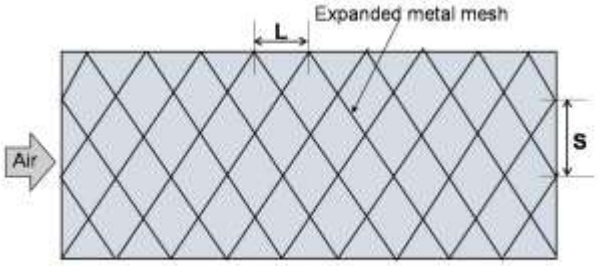 Expanded Metal mesh	MESH
[28]	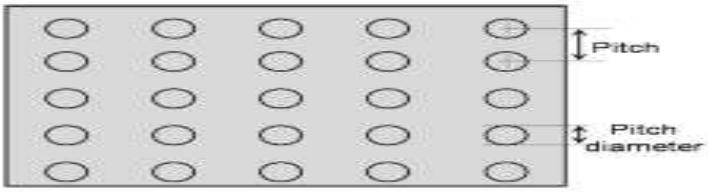 Absorber plate with Dimple-shaped geometry	DIMPLE
[29]		
[30]	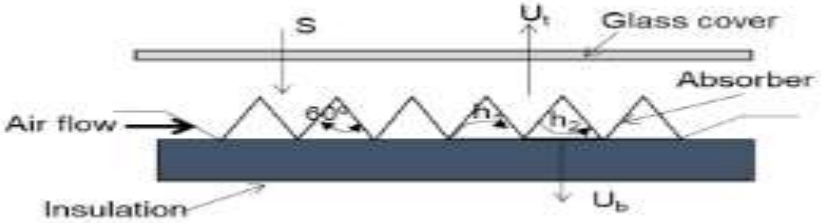	Triangular
[31]		Wave
[32]	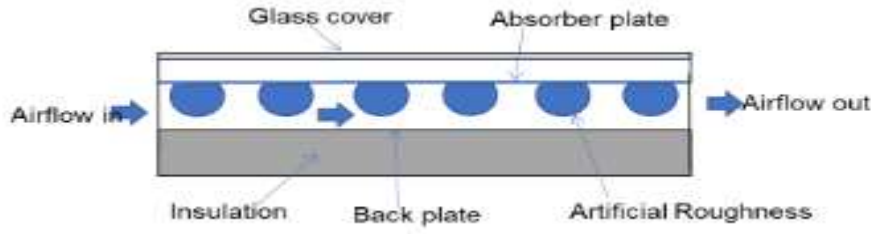	Circular

[33]		Dimple
[30]	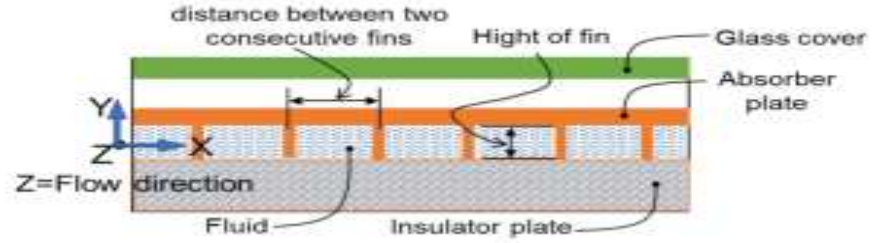	Novel design
[24]	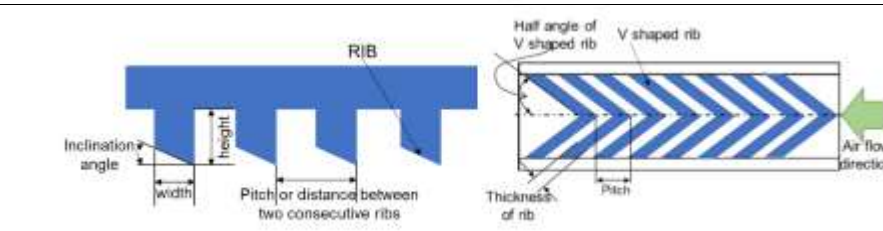	Vshaped
[34]		V shaped
[35]	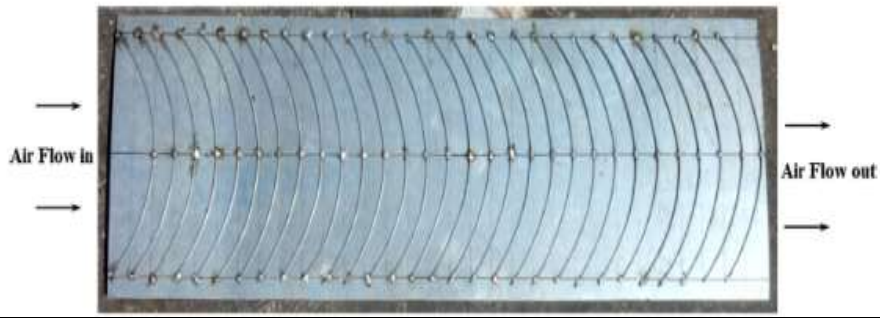	U shaped

The development of hybrid nanomaterials is still in its beginnings. A vast array of nano materials and black paint combinations must be researched in order to produce the optimum results. By harmonizing thermophysical properties with synergistic interactions, it is feasible to attain the optimum outcomes. With the correct synthesis and characterisation, a broad range of permutations and combinations are feasible. The pairing of a high-performing individual entity with a lower-performing counterpart in the correct mix may generate fascinating effects. New research possibilities have been opened up due of the thermophysical compatibility of the hybrid nanomaterial selective coatings.

Effect of rib/baffle height on THP

The ultimate purpose to introduce artificial roughness in the form of ribs or baffles is to interrupt laminar sub-layer and induce turbulence in the flow[36]. The rib or baffle height must be chosen in such a way that the ribs or baffles are able break the sublayer and should not increase the pressure drop unduly. The rib or baffle height is often given in dimensionless form. To convert height in dimensionless form, it is divided by either hydraulic diameter or height of duct. $,H\text{-}rrh.$and $,H\text{-}rbh.$ are the symbolic representation provided to relative rib and relative baffle height respectively. In Table 1, the optimum values of $,H\text{-}rrh.$and $,H\text{-}rbh.$ evaluated by researchers in past studies have been mentioned. The height of artificial roughness give rise to flow separation as seen in Fig. 3. The

flow separation and subsequently reattachment decides the rate of heat transfer[37]. The relative height of rib is notably low as comparing with the height of baffles, cited Table 1. The height of baffle is 5-10 grater that height of rib, see Table 1. It is pretty clear from Fig. 3, that the turbulence is larger near the wall of roughness when the height is more but the reattachment of fluid is not correct. This behavior leads to decrement in heat transfer while the pumping power need increases dramatically, and consequently THPP drops. To increase the THPP, the roughness height must be adjusted optimum with relative pitch.

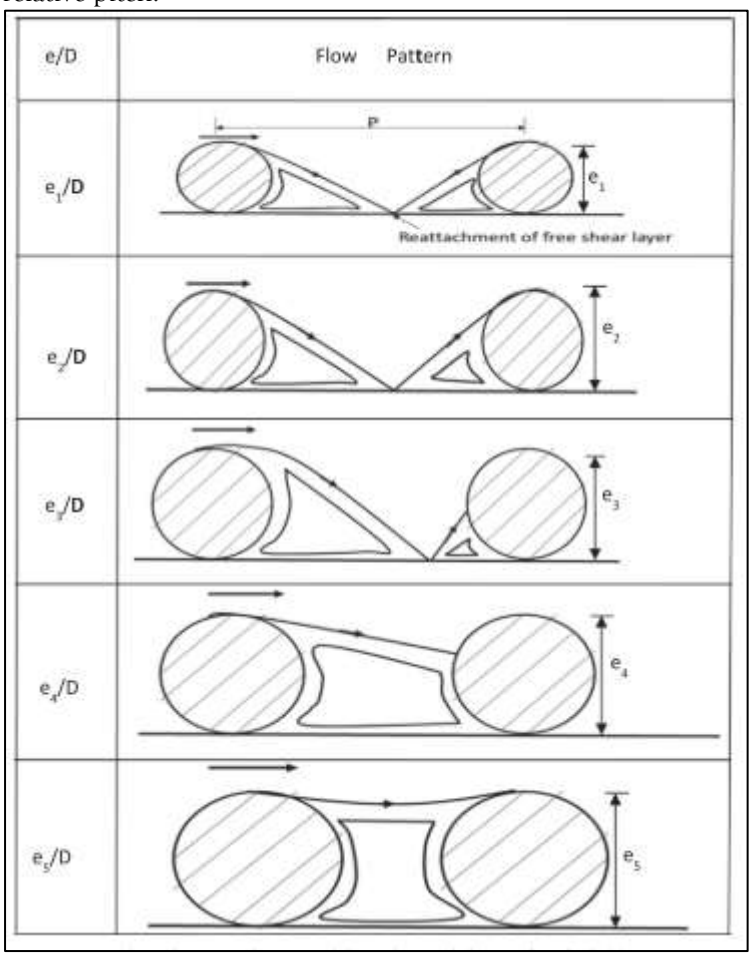

Fig.3. Effect of roughness height on flow[37]

2.2 Effect of rib/baffle pitch on THPP

It may be concluded from prior discussion that the relative roughness height in combination with relative roughness pitch, dominantly impacts the THPP. The spacing between two subsequent ribs/baffles has been defined as pitch. The pitch likewise relative roughness height also has been described in terms of dimensionless form. To make the value dimensionless, pitch value is commonly divided by height of rib/baffle (,*P-rrp*.=,,*P-rib*.-,*e-rib*.).. The relative roughness pitch (,*P-rrp*.&,*P-rbp*.) depends on height of rib/baffle. The relative roughness pitch should not be low as well should not be excessive. The explanation is that the ribs/baffles are placed too closely at lower value of pitch and thus reattachment zones are not produced. Due to this heat transfer is lowered while pressure drop increases. Owing to this behaviour, THPP reduced dramatically. For increasing value of relative roughness pitch, the number of reattachment zones decreased and consequently, heat transmission lowers albeit pressure drop has also dropped. The decrease in the heat transfer, lowers down the THPP. Table 1, represent the optimal value of relative roughness pitch in both the circumstances i.e. when ribs and baffles have been applied.

Table 1 Artificial roughness relative height used for ribs and baffles

Ribs		Baffles	
SK Sharma and VR Kalamkar[38]	H_{rrh}= 0.055 $P_{rrp} = 10$	F. Chabane et al[39]	H_{rbh}=0.5 $P_{rbp} = 5$

AZ Aghaie et.al [40]	H_{rrh}= 0.05 − 0.75 $P_{rrp} = 1 - 2$	A Kumar and MH Kim[41]	H_{rbh}=0.6 $P_{rbp} = 8$
D. Jin et al.[42]	H_{rrh}= 0.043 $P_{rrp} = 10$	S Sharma et al.[43]	H_{rbh}=0.5 $P_{rbp} = 10$
Jain et.al [44]	H_{rrh}= 0.043 $P_{rrp} = 10$	P.T Sarvanakumar et al.[45]	H_{rbh}=0.0422 $P_{rbp} = 10$
Y.M Patel et.al [46]	H_{rrh}= 0.043 − 0.87 $P_{rrp} = 5 - 13.33$	B.Sahin et.al [47]	H_{rbh}=0.25-0.38 $P_{rbp} = -$

2.2 Effect of rib/baffle shape on THPP

The shape of rib/baffle has also play crucial function in the enhancement of THPP apart from relative height and relative pitch. The shape and magnitude of vortices varies upon the surface over which the fluid is flowing. In the approaching part, author has tried to summarize the common shapes of roughness elements that has been employed as rib as well as baffles.

2.2.1 Transverse

The ribs are first inserted in transversely as reported in past research. The Prasad and Mullick[48] has installed tiny diameter wire in the transverse direction. The effectiveness of SAH was enhanced by14% when relative rib height (,*H-rrh*.) and Relative rib pitch (,*P-rrp*.) was retained at 0.019 and 12.7 respectively at Re=5000. Prasad and Saini[49], carried out the same work further and produced correlations for Stanton number and average friction factor by altering (,*H-rrh*.) and (,*P-rrp*.) as 0.020-0.033 and 10-20 respectively. The results demonstrated that Nu and f were strongly reliant upon (,*H-rrh*.) and (,*P-rrp*.). The Nu and f increased with the growth of ,*H-rrp*..But, Nu reduced and f increased with the growth of ,*H-rrh*..Gupta et al. [50] has performed studies to see the effect of Re, duct aspect ratio, relative roughness height ,*H-rrh*. and relative rib height (,*H-rrh*.). The relevant range of these parameters were taken as 3000-18000, 6.8-11.5, 0.018-0.052 and 10 respectively. The largest enhancement in Stanton number was seen at Re=12000. Sahu and Bhagoria [51] performed experimental research on 900 broken transverse ribs. The pitch of rib was modified from 10-30 mm while rib height and duct aspect ratio was kept fixed at 1.5 mm and 8 correspondingly. The Re was varied in the range of 3000-12000. The results have showed that the greatest value Nu was found at Re=5000 and Pitch=20 mm. The heat transfer has been seen increasing with addition of transverse ribs. The researchers in the same time has been trying to implement baffles of equal shape across the SAH.

Similar to ribs, baffles are likewise inserted in the same way. Ho-Ming Yeh and Wen Hsen Chou[52] have completed studies to estimate collector efficiency utilizing fins and baffles. The studies concluded that baffles increased the turbulence as well as the heat transmitting regions. The density and location of baffles improved both pressure drop and collector efficiency. M.A.Al-Nimr and R.A.Damesh[53], provided a mathematical model that explained the dynamic thermal behaviour of baffled SAH. The validation of mathematical model has been done by completing experiments. The intensity of solar light and fluid temperature were the factors evaluated for experimentation work. The conclusion of the investigation resulted in three design characteristics that regulated the performance of baffles SAH.

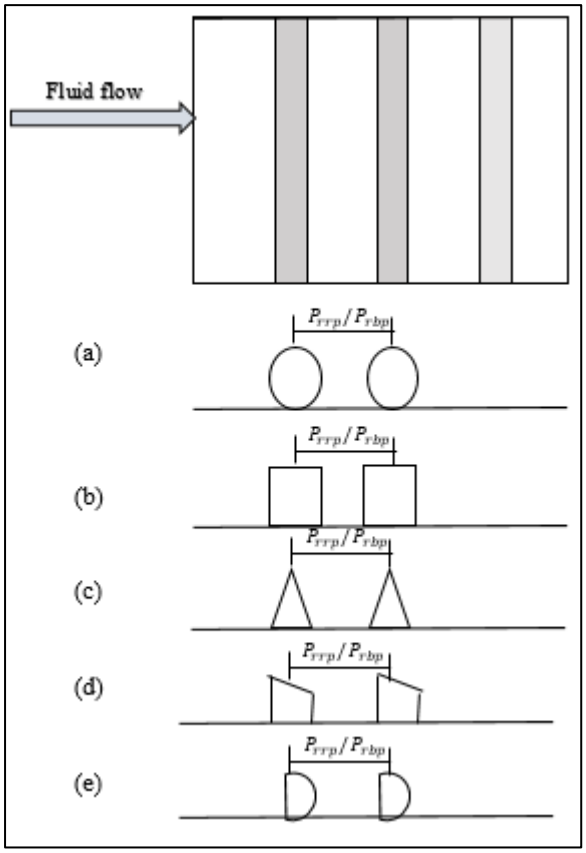

Fig.3. Cross sections of transverse ribs/baffles (a) Circular (b) Square (c) Triangular (d) Forward chamfer (e) Quarter circular

2.2.2 Inclined transverse

The studies on transfer ribs further extended to tilted the ribs. Gupta et al.[54] has employed inclined ribs and angle of inclination has been kept fixed at ,60-0. while ,H-rrh.has varied from 0.023 to 0.5 and ,P-rrh.=10. Inclined ribs has depicted in Fig. 4. An enhancement of 1.16-1.25 in thermal efficiency of roughened SAH over smooth SAH has been discovered. Aharwal et.al.[55], has evaluated influence of slanted ribs with gaps on the performance of SAH, Fig. 5. The values of ,H-rrh. and ,P-rrh. have been kept fixed at 0.0377 and 10 respectively while the relative rib gap width and relative position of gap has been altered. The value of Nu and f for roughed SAH have been determined 2.59 and 2.87 time more than smooth SAH. In the next experimental work, Aharwal et.al.[56] instead of relative rib gap width and relative position of gap, has adjusted other parameters also. The parameters were angle of attack, ,H-rrh. and ,P-rrh.. The operational range were taken as ,H-rrh.=0.018—0.0377, ,P-rrh.=4—10 and angle of attack ,30-0.—,90-0.. The maximum augmentation in Nu and f for roughed SAH have increased to 2.83 and 3.63 respectively.

Similar to inclined ribs, P. Dutta and A. Hossain[57], have evaluated the influence of inclined solid and perforated baffles on the performance of SAH, see Fig, 6. The influence of shape, position and orientation of baffles have been examined and results revealed that Nu of roughened SAH was found to be raised by 4.8 time than smooth SAH. The f of roughened SAH has likewise risen to maximum 11 times than smooth SAH. P. Promvonge et al.[58], quantitatively examined the influence of ,45-0. tilted baffles on the performance of SAH. The operating parameter was ,H-rbh. and ranged from 0.1-0.5. The results have been compared with the performance of SAH with transverse baffles. The value of Nu has greatly increase when comparing with transverse baffles case

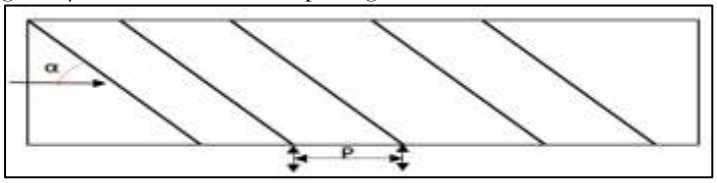

Fig.4 Inclined continuous ribs[54]

International Journal of Environmental Sciences
ISSN: 2229-7359
Vol. 11 No. 8, 2025
https://theaspd.com/index.php

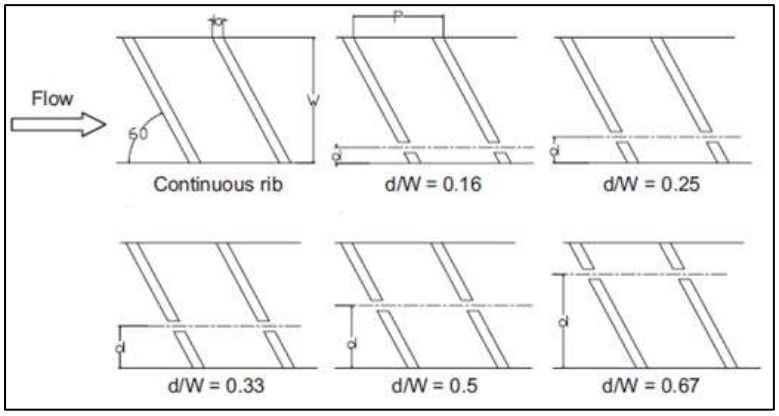

Fig. 5 inclined ribs with gaps[55]

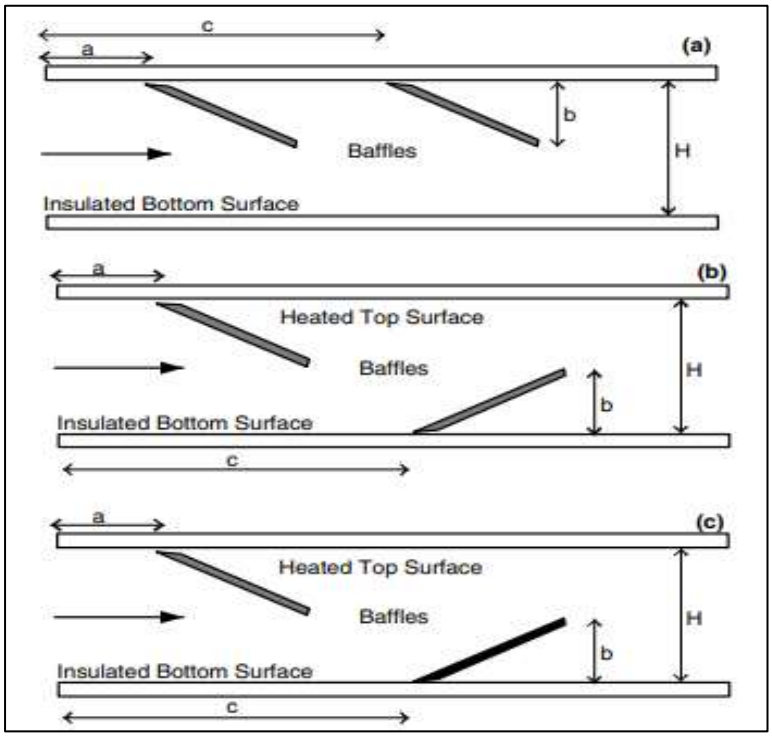

Fig. 6 Inclined baffles[57]

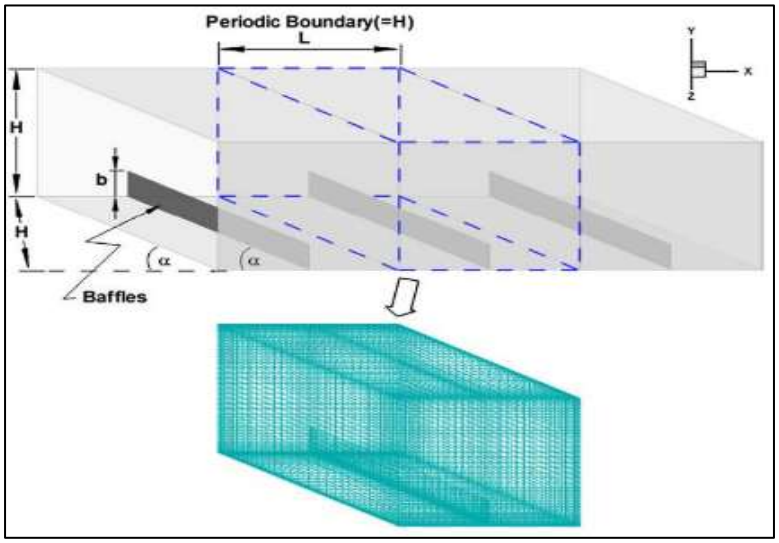

Fig. 7 Inclined baffles at 45^0[58]

2.2.3. Arc Shape

Researchers has observed that the inclined transverse ribs and baffles have resulted in greater performance then transverse ribs and baffles. One of the likely factors for the performance boost was the production of cross flow. Researchers further restructured the inclined shape into arc shape.MK Sahu and RK Prasad [58], quantitatively examined the performance of SAH when arc shape ribs have been added on backside of SAH. The MATLAB software has been used to solve the mathematical model. The angle of attack=0.333-0.666, ,H-rrh.=0.0213—0.0422 and ,P-rrh.=10 were the parameters of investigation. The thermal efficiency of the roughened SAH was determined at 79.84%. AP Singh et al.[59], has carried out experimental investigation on thermo-hydraulic performance of SAH containing numerous arc shape ribs. The operating parameters with range were Reynolds number 2200-22000, ,H-rrh.=0.018—0.045, ,P-rrh.=4-16, arc angle ,30-0.—,75-0. and relative roughness width 1-7. The maximum THP was found to be 3.4. NK Pandey et al.[60], has experimentally evaluated the performance of SAH in terms heat transmission and friction factor features utilizing numerous arc shape ribs with gaps, Fig. 10. The investigation has comprised of following parameters: Re=2100-21000, ,H-rrh.=0.016—0.044, ,P-rrh.=4-16, arc angle ,30-0.—,75-0., relative roughness width= 1-7, gap distance(relative)=0.25-0.85 and gap width(relative)=0.5-2. The maximal augmentation in Nu and f found to be 5.85 and 4.96 respectively.

Inline to arc form ribs, various researches on arc shape baffles have been documented. N Koolnapadol et al.[61], has researched the behaviour of SAH having arc shape baffles turbulators(ASB) on heat absorption surface. The, P-rbh. has varied from 4-8 and thermochromics liquid crystal has been utilized to explore the contours of temperature and Nu. The heat transfers of SAH with baffles was found to be improved by 127% in-comparison to smooth SAH. P. Saravanakumar et al.[62], has incorporated arc shape ribs with baffles and fins and evaluated the thermohydraulic performance of SAH, see Fig. 11. The analytical approach has been carried out by considering width and length of baffles, Reynolds number and number of fins. The thermal efficiency of SAH with fins, ribs and baffles has been found raised by 28.3% in-comparison with SAH with ribs.

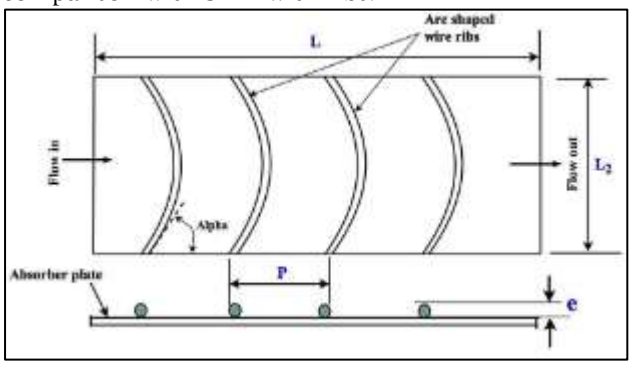

Fig.8 Arc shape ribs[58]

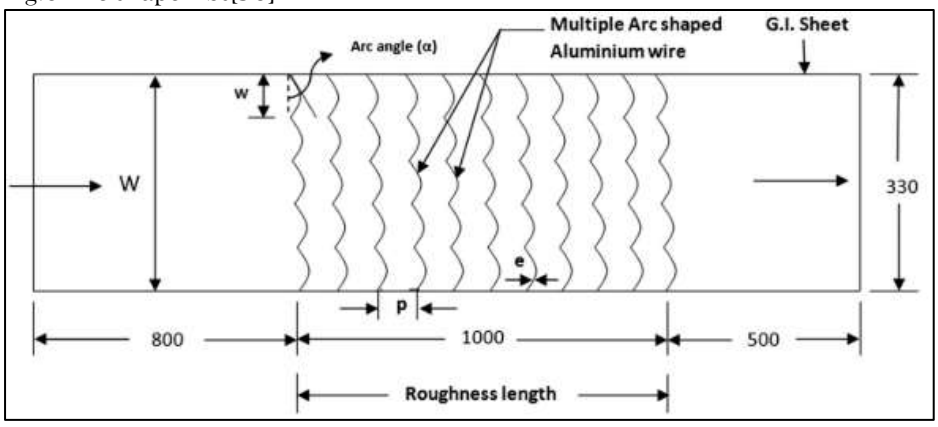

Fig. 9 Multiple arc rib[59]

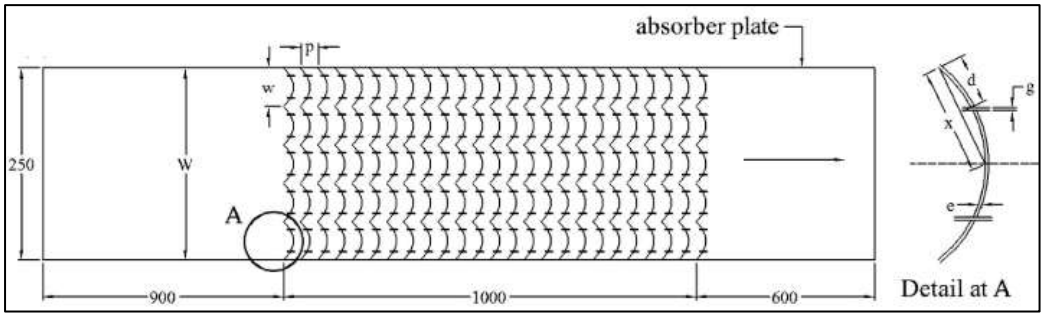

Fig.10 Multiple arc ribs with gaps [60]

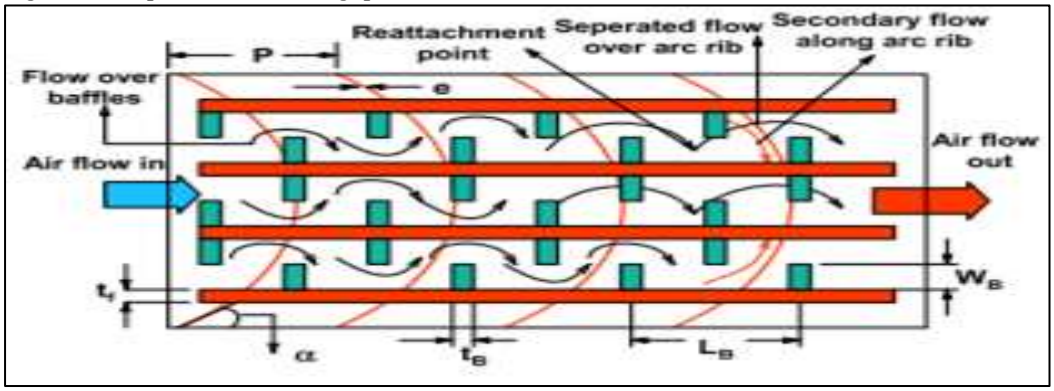

Fig.11 Arc shape ribs integrated with baffles[62]

2.2.4. S- Shape

K. Kumar et al.[63], performed experimental analysis on the performance of SAH having S shape ribs. The tested operating parameters were: Re=2400-20000, ,H-rrh.=0.022—0.054, ,P-rrh.=4-16, angle of attack ,30-0.—,75-0. and relative width 1-4. The greatest enhancement in THP was determined to be 3.34. The gap within the ribs has offered greater results, as noted in proceedings section. Owing to this, D. Wang et al. [64] has carried out experimental analysis of the performance of SAH roughened with S-shape ribs with gap. The operational parameters were: Re from 2000-20000, ,H-rrh.=0.023—0.036, ,P-rrh.=20-30, relative roughness width 3-5, relative gap 1-2. The maximal augmentation of Nu and f was found to be 5.42 and 5.87 when compared with smooth SAH. In the literature, no research has been discovered that incorporated S shape baffles. But, S. Sharma et al.[43], has published the performance evaluation of SAH with sine wave type baffles which has resemblance of S shape. The numerical research was conducted by considering following parameters: Re=4000-16000, angle of attack= ,0-0.—,45-0. whereas, ,P-rbh. was kept fixed at 10. The greatest THP attained was 1.6.

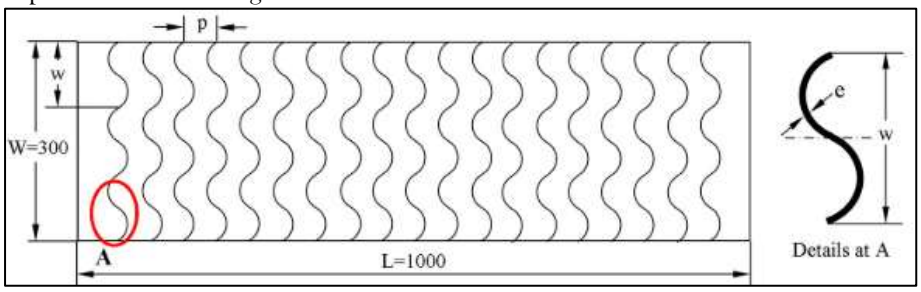

Fig. 12 S shape ribs[63]

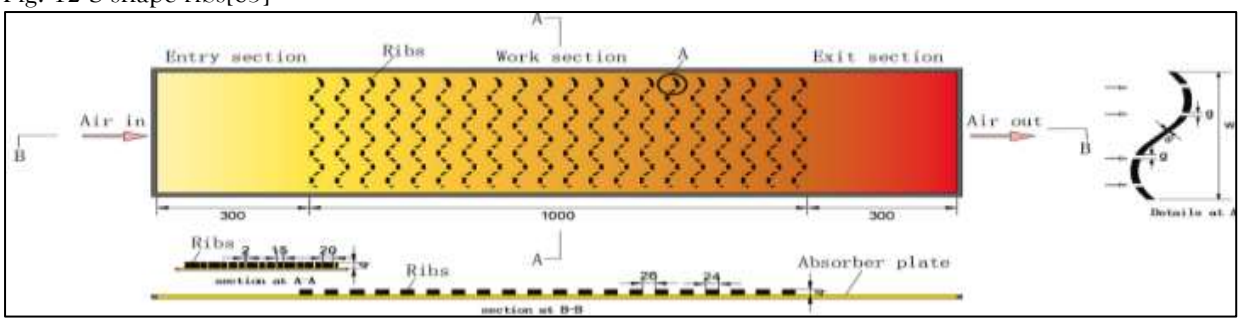

Fig. 13 S shape ribs with gaps[64]

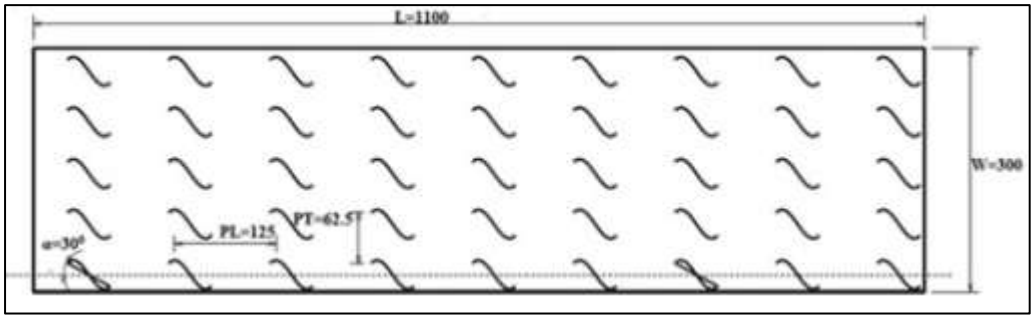

Fig. 14 Sine wave baffles[43]

2.2.4. V Shape

The influence of V shape ribs was researched by several scholars. JC Chan et al.[65], has performed experiment on rectangular channel employing nine configuration of ribs. The configurations have displayed in Fig. 15 and findings revealed that the largest augmentation in heat transport has attained by using V shaped ribs. R Maithani and JS Saini [66], performed experiments on SAH utilizing V ribs having symmetrical spacing, see Fig. 16. The THP has determined by maintaining ,P-rrh. and ,H-rrh. and angle of attack fixed at 10, 0.0433 and 600 correspondingly. The relative gap width (g/e) and number of gaps (Ng) were altered and range of variations was kept identical 1-5. The greatest THP was reached at g/e=4 and Ng=3.D Jin et al.[67], has undertaken numerical investigation by inserting inline and stagger V ribs on absorber plate. The 3D analysis has been performed by adjusting following parameters: Re, stagger distance; ,P-rrh., ,H-rrh.and attack angle. The results revealed that staggered V ribs has resulted in highest augmentation of Nu in-comparison to inline V ribs. Corresponding to maximum Nu, staggered V ribs have likewise resulted in maximum THP and the values of THP was 2.43. S. Chamoli and NS Thakur[68], have completed studies to evaluate the heat transmission and friction factor properties of SAH roughened with V-down perforated baffles, Fig 18. The experiments were performed by taking following parameters: Re=3800-19000, ,P-rbh.=1-4, ,H-rbh.=0.285—0.6 and open area ratio12-44%. The remarkable improvement in the Nu and f have been reported. SK Jain et al. [69], have installed distinct V shaped perforated baffles on SAH and the THP, Fig 19. The effect of Re=4000-18000, ,P-rbh.=6, ,H-rbh.=0.3—0.6, open area ratio 23% and angle of attack 600 have been examined. The highest augmentation of THP was seen at ,H-rbh.=0.4 and the values was 2.4. A. Kumar et al.[70], has undertaken experiments on SAH with numerous V-down pattern perforated baffles placed an angle of 600, Fig. 20. The THP of SAH has determined by adjusting Re from 4000-9000, ,P-rbh.=10, ,H-rbh.=0.5, relative hole position 0.44 and open area ratio at 12%. The studies have indicated that V perforated baffles had greatest THP relative to all other forms and maximum value attained was 3.41.

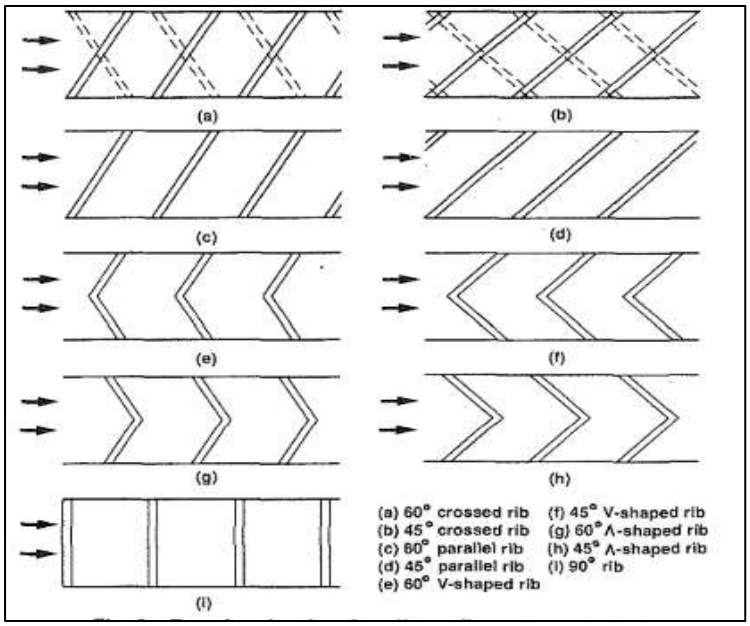

Fig. 15 V shaped ribs[65]

International Journal of Environmental Sciences
ISSN: 2229-7359
Vol. 11 No. 8, 2025
https://theaspd.com/index.php

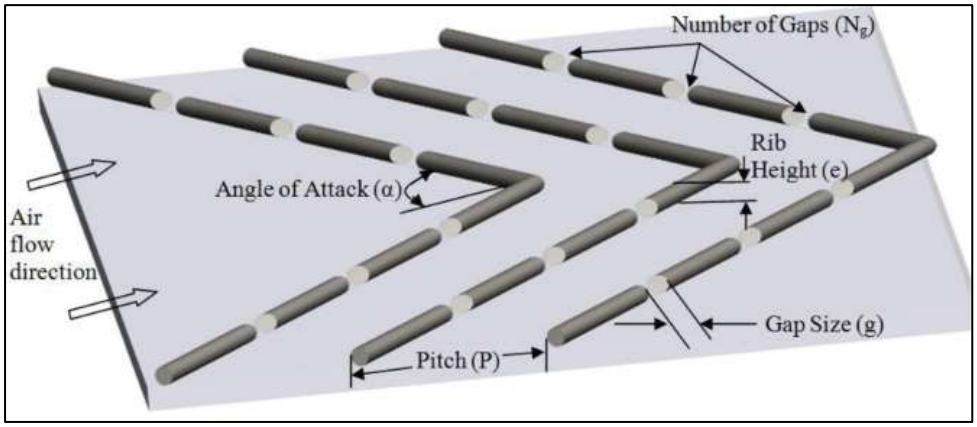

Fig. 16 V ribs with gap[66]

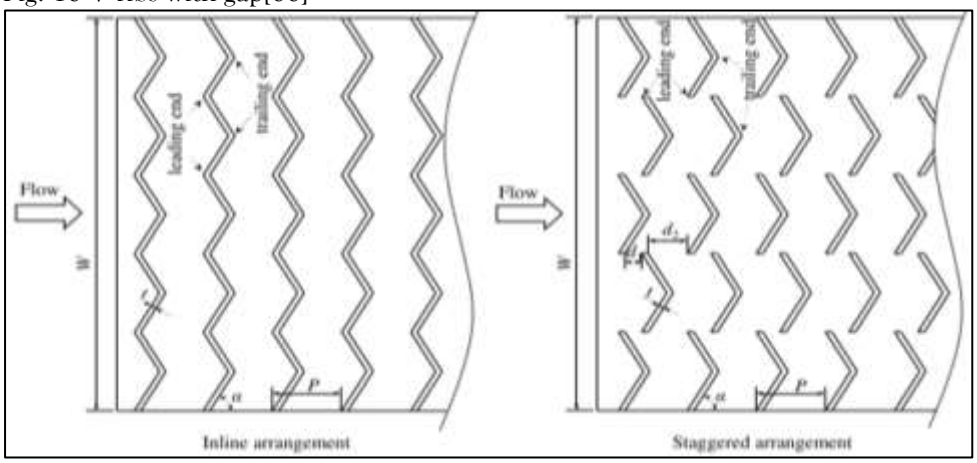

Fig. 17 Multiple inline and Staggered V ribs[67]

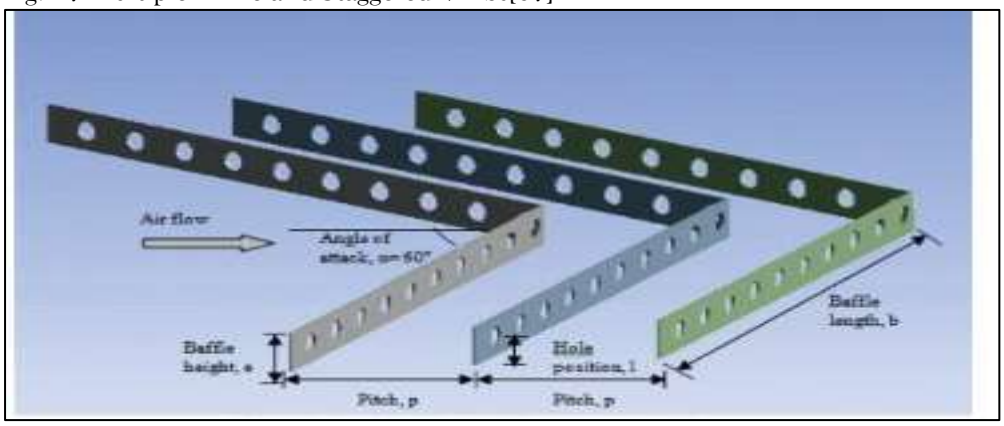

Fig. 18 Single V perforated baffles[68]

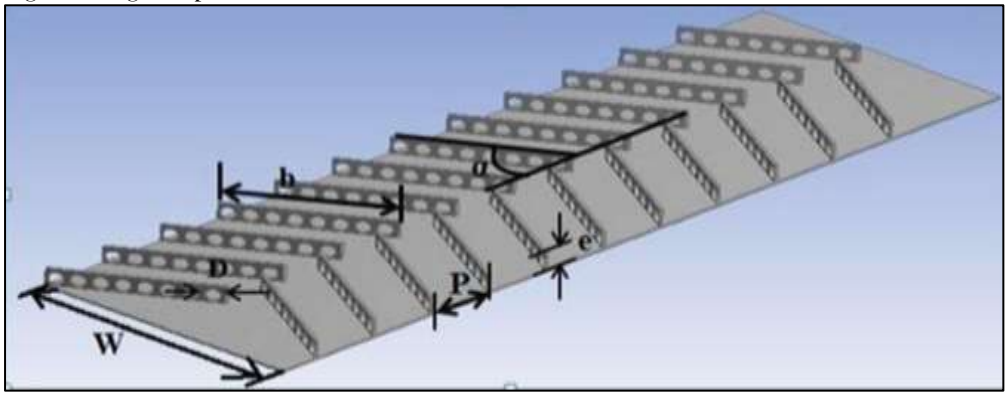

Fig. 19 V discrete perforated baffles[69]

Fig. 20 V perforated baffles[70]

2.2.5 Other types of ribs and baffles

Apart from these ribs/baffle shapes, numerous more shapes have also been used by researchers. These shape have resulted in higher performance of SAH. The author has endeavored to incorporate several of these rib/baffle shapes in the present analysis. The shapes have been employed either rib or baffle, however none of these shapes typically utilized as rib and baffles. The other rib shapes are Dimple[71], L shape[72], Mesh[73], Metal grid[74], NACA[46], Twisted[75], U[76], W[77], [78] etc.

RP Saini and J Verma[71], have completed studies on SAH employing dimple shape ribs, Fig. 21. The heat transmission and friction factor characteristics have been examined by adjusting Re from 2000 to 12000, ,P-rrh.=8-12 and ,H-rrh.=0.018—0.037. The greatest value of Nu has obtained at ,P-rrh.=10 and ,H-rrh.=0.037 whereas, minimum value of f has obtained at ,P-rrh.=10 and ,H-rrh.=0.0289. V. B. Gawande et.al[72], has completed both numerical and experimental research to access thermal performance of SAH roughened with L shape ribs, Fig. 22. The studies have been carried out by keeping ,H-rrh.=0.042 fixed, although other parameters i.e. Re and ,P-rrh. have varied and respective variation ranges were 3800-18000, 7.14-17.86. The THP has dramatically increased and has reached at value of 1.9. RP Saini and JS Saini[73], have undertaken studies on rectangular channel by using metal mesh ribs. The heat transmission and friction factor characteristics were examined by altering ,H-rrh., Re, relative longway and shortway length of mesh. The range of parameters were: ,H-rrh.=0.012—0.039, Re=1900-13000, relative longway length= 25-71.87 and shortway length=15.62-46.87. The maximum increment in Nu and f were 4 and 5 respectively,

SV Karmare and AN Tikekar[74], have utilized metal grit ribs on the absorber plate to enhance the thermal performance of SAH. The studies have been conducted by altering relative length of grits(l/s), Re,,P-rrh. and ,H-rrh. while the aspect ratio of duct is kept at 10:1. The ranges of variable parameters were: l/s=1.72-1, Re=4000-17000, ,P-rrh.=12.5—36 and ,H-rrh.=0.035—0.044. The largest enhancement in performance has noticed at l/s=1.72, ,P-rrh.=17.5 and ,H-rrh.=0.044. YM Patel et al.[46], has performed studies to investigate the performance of SAH by putting NACA0040 shape ribs in reverse order. The operating parameters with operating range were: Re=6000-18000, ,P-rrh.=5—13.33 and ,H-rrh.=0.043—0.087. The maximum THP has found to be 2.53. A. Lanjewar et al.[78], has carried out experimental research to boost the performance of SAH roughened with discrete W shape ribs. The value of ,P-rrh. been kept fixed at 10 while the other variables have altered. The other parameters with the ranges were: Re=3000-15000, ,H-rrh.=0.0168—0.0388 and angle of attack 300-750. The maximal augmentation of Nu and f has been observed 2.16 and 2.75 respectively.

Baffle of other odd shapes have been employed in literature. The baffles of Curved perforated[79], Plus shape[80], Wave like[81], Z shape[82] etc.

EL Said[79], has used several curved baffles to boost performance of double pass SAH. The numerical experiments have been carried out on CFDRC program by adjusting diameter of hole, inclination angle of baffles and mass flow rate of air. The thermal efficiency greatly enhanced with the usage of curved perforated baffles and obtained value of 77%. A. Khanlari et al.[80], has carried out experimental and numerical analysis to study the effect of the plus shape baffles on the performance of SAH. The investigations were performed by considering following configuration: Single pass collector without Single baffle (PPSCB), parallel pass solar collector with double baffles(PPSCDB) and the performance has been compared with parallel pass solar collector without baffles(PPSC). The influence of mass flow rate in addition to shape has also been investigated. The results revealed that the PPSCDB configuration has resulted in maximum thermal efficiency at greater mass flow rate. JJ Fluk and k. Dutkowski[81], have employed three wavelike baffles sheets on the absorber surface to boost thermal efficiency of SAH. The

studies were conducted by considering three instances i.e. 1. Without baffles 2. Baffles arranged continually 3. Placing middle sheet in reverse order. The maximum thermal efficiency of 73.8% has been reached in 2nd situations i,e. without sheet reversing. P. Sriromreun et al.[82], has numerically and experimentally evaluated the effect of zigzag baffles(Z shaped) put in sequence over the absorber plate on the performance of SAH. The operational settings and the ranges were: Re=4400-20400, ,P-rbh.=1.5—3, ,*H*-rbh.=0.1—0.3 and baffles were arranged at 450 angle. The results showed the presence of Z shaped baffles has improved the performance of SAH,

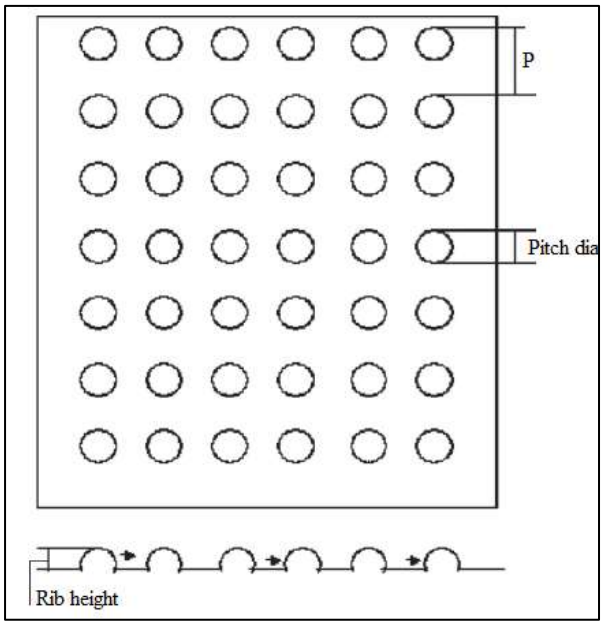

Fig.21 Dimple shape ribs[71]

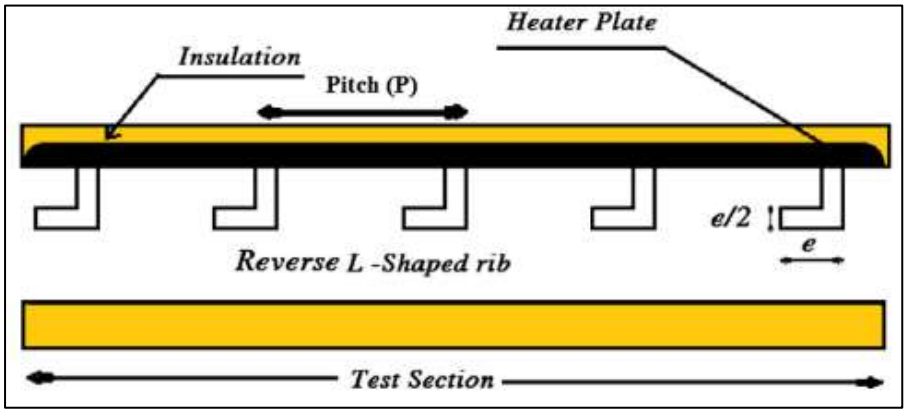

Fig.22 L shape ribs[72]

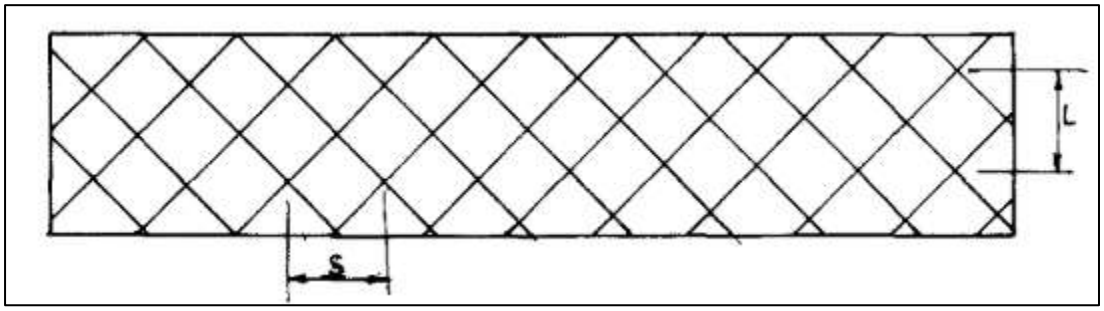

Fig.23 Mesh ribs[73]

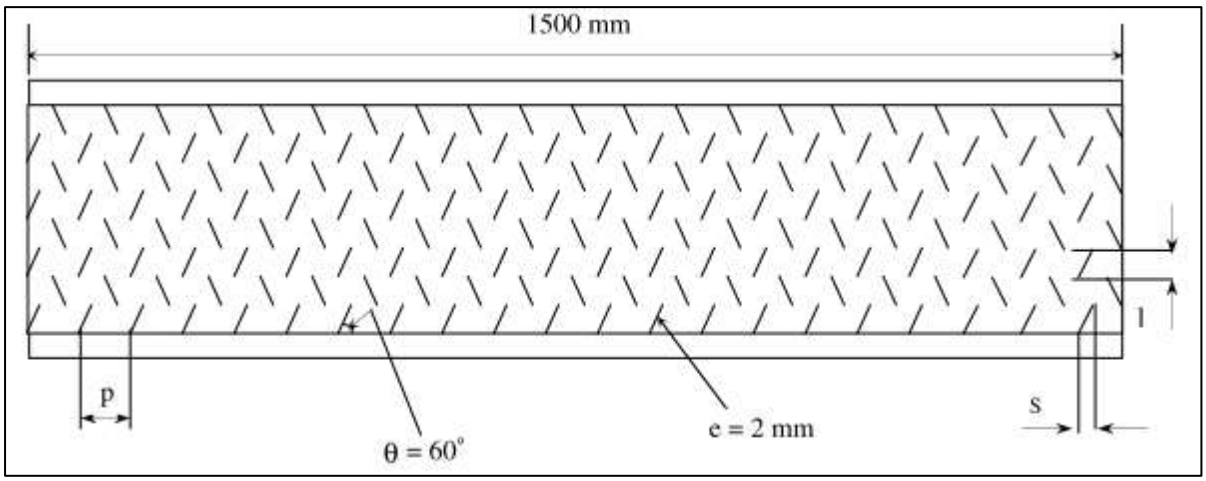

Fig.24 Metal grits ribs[74]

Fig.25 NACA ribs[46]

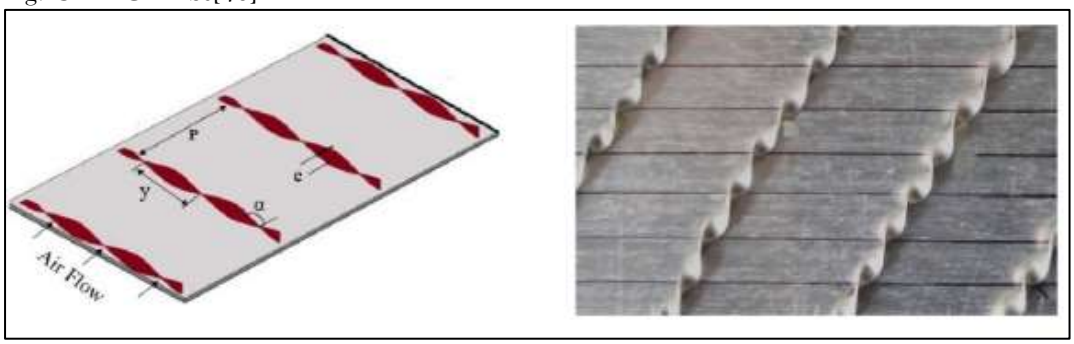

Fig. 26 Twisted tape[75]

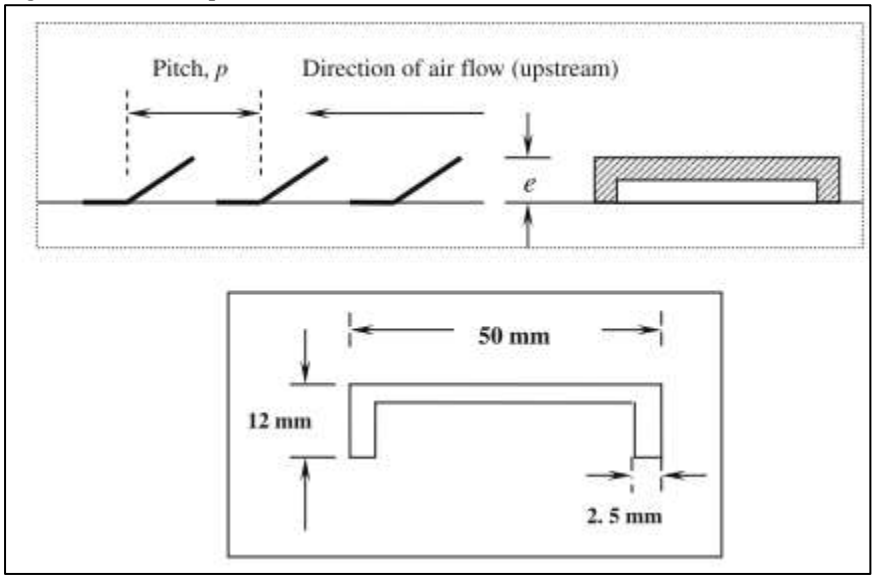

Fig. 27 U shape rib[76]

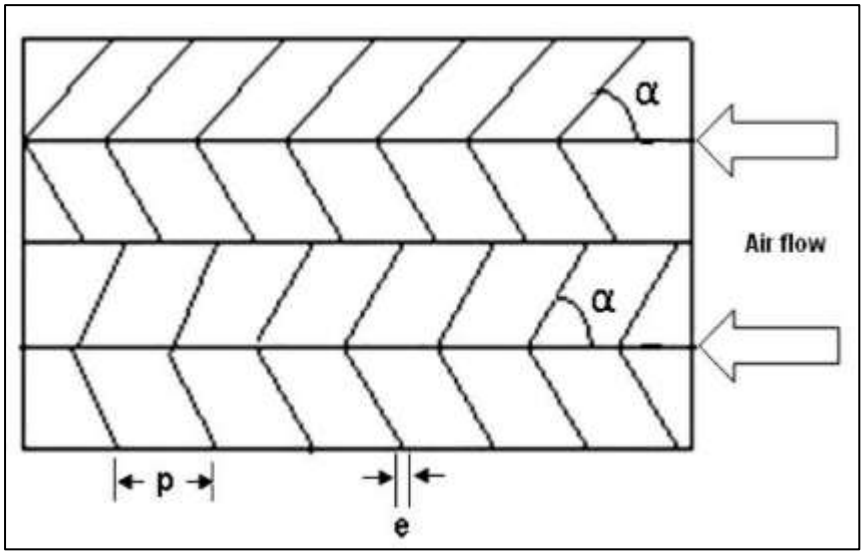

Fig. 28 Discrete W rib[77]

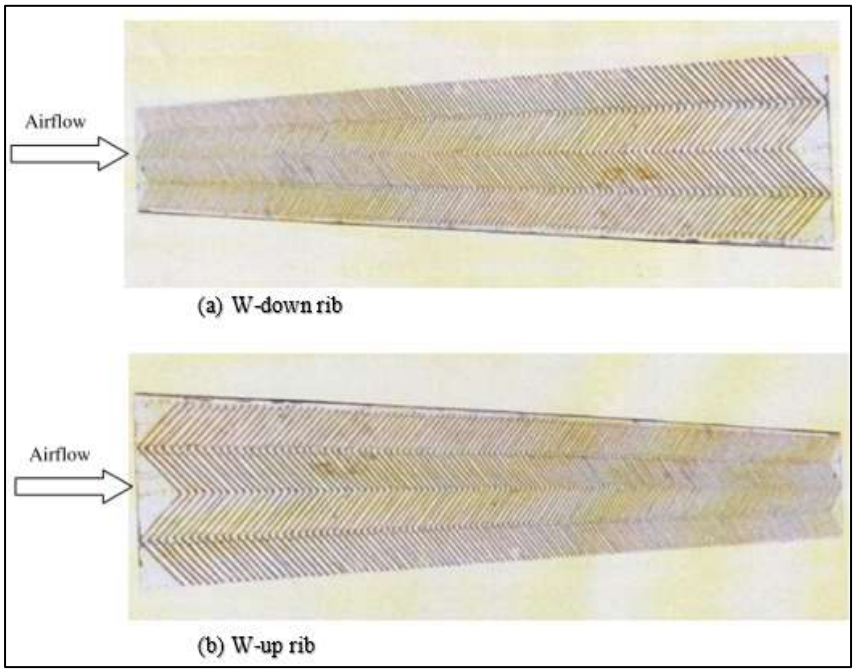

Fig. 29 W shape rib[78]

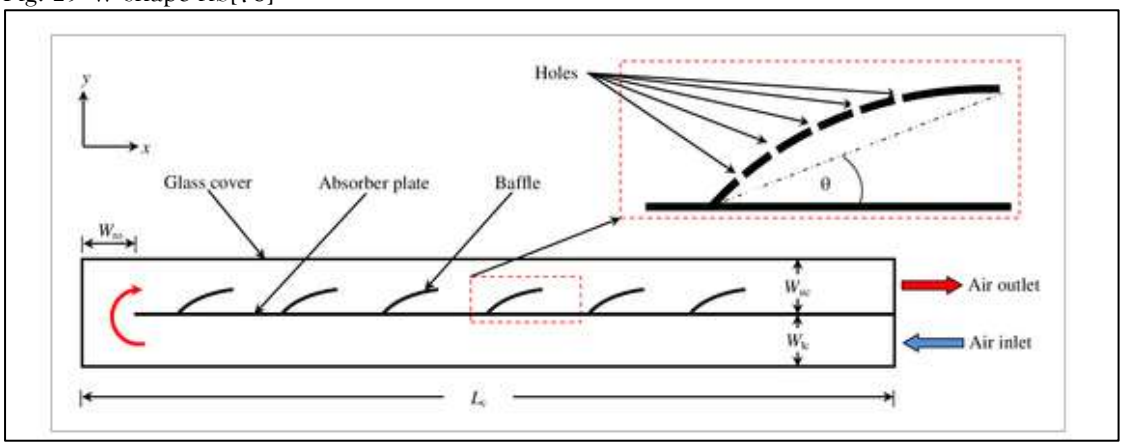

Fig. 30 Curved perforated baffles[79]

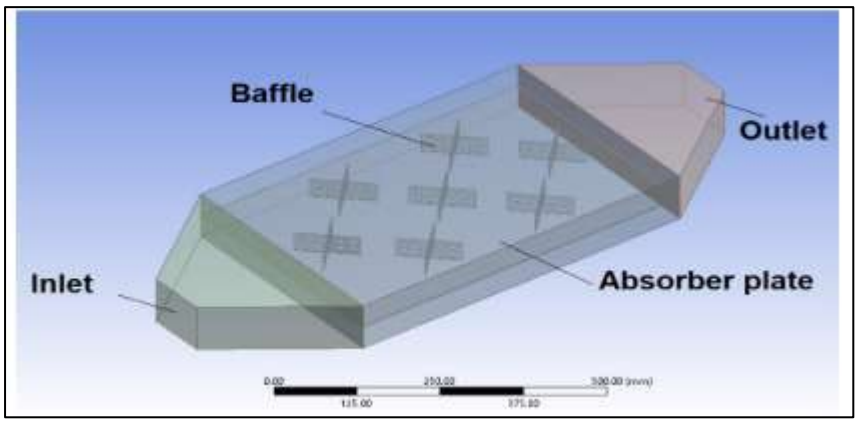

Fig. 31 Plus shape baffles[80]

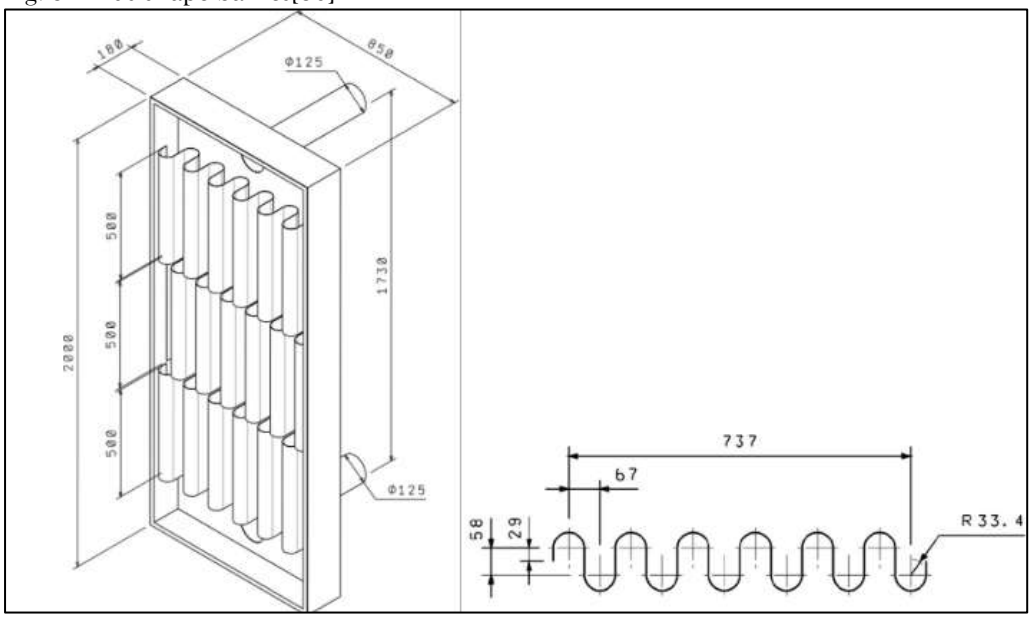

Fig. 32 Wave like baffles[81]

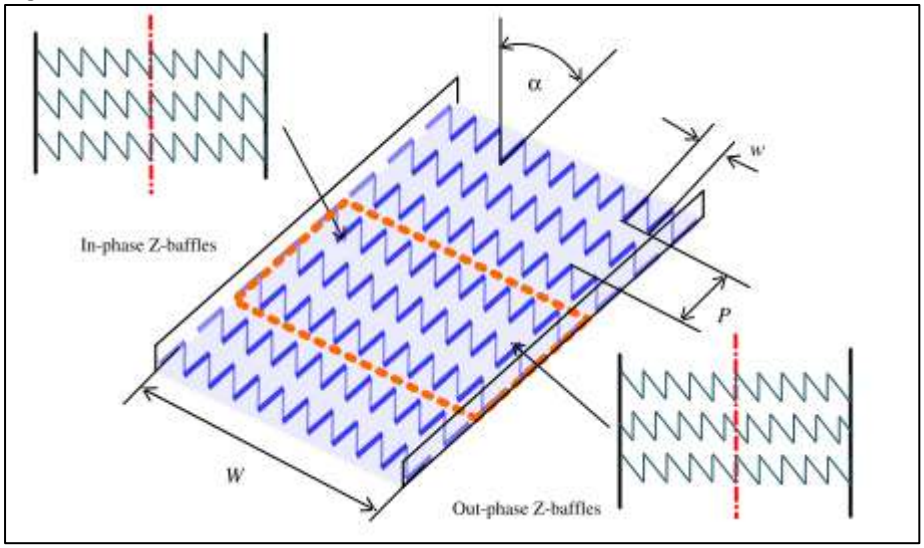

Fig. 33 Z shape baffles[82]

2.4 Effect of rib/baffle orientation on THPP

It is pretty obvious from prior discussion that the rib/baffle form with relative height and pitch have substantial effect on the THP. The rib/baffle inclination is another essential component that likewise has dominating effect on the Nu and f. The development of vortices depends upon the rib/baffle positioning against the flow. The size pf vortices have been modest and smaller in quantity when ribs/baffles have

been placed parallel to flow[36] . The inclination of ribs/baffles against the flow give birth to the secondary flow[83]. This secondary flow along the along the ribs/baffles get integrated with the primary flow and consequently, heat transfer improved. However, this secondary flow some time deceases the THP because of increased pumping power requirement[84]. The various experimental and numerical research have documented in literature proposing that how to select optimum inclination angle with optimum rib/baffle height and pitch[85]–[88]. The primary findings for various ribs and baffles have been given in Table 2.

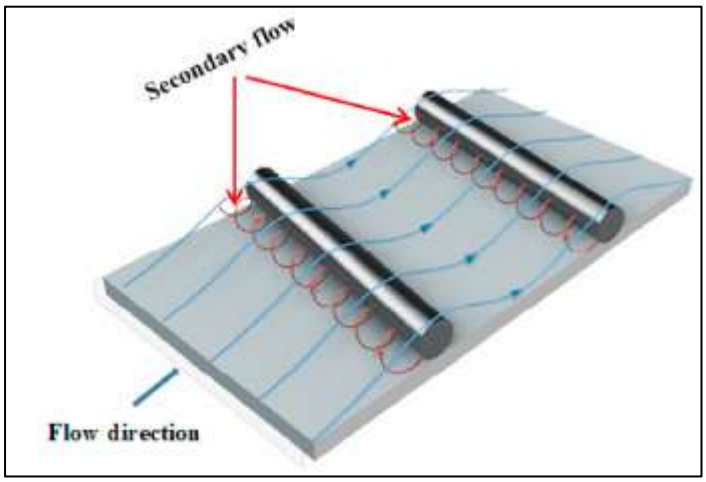

Fig. 33. Effect of rib/baffle orientation[36]

Table 2. Major findings reported for various ribs and baffles

Ribs					
Shape	Investigator	Parameters	Nu_{rough}/Nu_s	f_{rough}/f_s	THP or Thermal efficiency (%)
Forward chamfer	R.Kumar et al.[89]	$H_{rrh}= 0.024-1.5$ $P_{rrp}=12$	2.88	2.64	
NACA0040	YM Patel et al.[46]	$H_{rrh}= 0.065$ $P_{rrp}=5$			1.69-2.53
S Shape	K. Kumar et al.[63]	$H_{rrh}= 0.022-0.054$ $P_{rrp}=4-16$	4.64	2.71	3.34
S Shape with Gaps	D. Wang et al. [64]	$H_{rrh}=0.023-0.036$, P_{rrh}=20-30	5.24	5.87	
Square	I.Singh and J.Singh [90]	$H_{rrh}= 0.043$ $P_{rrp}=4-30$			1.43
Circular	Y. Mahanand and J.R. Senapati [91]	$H_{rrh}= 0.042$ $P_{rrp}=7.14-17.86$			1.88
Triangular	Yadva and Bhagoria [92]	$H_{rrh}= 0.021-0.41$ $P_{rrp}=7.14-35.71$			2.06
V Shape	J.C Han et al.[65]	$H_{rrh}= 0.0625$ $P_{rrp}=10$	4.5	12	
Multiple V ribs with gaps	R. Maithani et al. [66]	$H_{rrh}= 0.043$ $P_{rrp}=10$	2.59	2.87	

Multiple V ribs	D Jin. et al.[67]	H_{rrh}= 0.022 − 0.087 $P_{rrp} = 6 - 20$			2.5
Baffles					
Arc	N. Koolnapadol et al. [61]				
Curved Perforated	Emad MS El Said[79]	$\theta = 7^0 - 27^0$			77%
Plus shape	A. Khanlari et al. [80]	PPSCDB			75.11
Sine wave	S. Sharma et al. [43]	H_{rbh}= 0.5 $P_{rbp} = 10$	2	10	1.6
Transverse	F. Chabane et al. [39]	H_{rbh}=0.5 $P_{rbp} = 5$			88%
V perforated	SK Jain et.al [69]	H_{rbh}= 0.3 − 0.6 $P_{rbp} = 6$	4.24	14.73	2.24
Multi V perforated	A. Kumar et al.[70]	H_{rbh}= 0.5 $P_{rbp} = 10$			3.41
Wave like	JJ Fluk et al. [93]				73.8%
Z Shape	P. Sriromreun et al. [82]	$P_{rbh} = 1.5 - 3$ $H_{rbh} = 0.1 - 0.3$			

Table 3. Correlation formed for various ribs/baffles

Rib shape	**Correlations**	**Major Findings**
Transverse[49]	$St = \frac{f/2}{1 + (4.5 * (e^+)^{0.28} Pr^{0.57} - 0.95 * (P/e)^{0.53})\sqrt{f/2}}$ $f = \frac{(W + 2B)f_s + Wf_r}{2(W + 2B)}$	-
V.B. Gawande et al. [102]	$Nu = 0.0943\ Re^{0.8248} \left(\frac{P}{e}\right)^{-0.3022}$ $f = 0.653\ Re^{-0.2823} \left(\frac{P}{e}\right)^{-0.2087}$	η_{th}=77% η_{eff}=70%
Inclined Transverse [103]	$Nu = 0.067\ Re^{0.888} \left(\frac{e}{D}\right)^{0.424} \left(\frac{\alpha}{60}\right)^{-0.077} \exp[-0.782 \ln\left(\frac{\alpha}{60}\right)^2]$ $f = 6.266\ Re^{-0.425} \left(\frac{e}{D}\right)^{0.565} \left(\frac{\alpha}{60}\right)^{-0.093} \exp(-0.719 \ln\left(\frac{\alpha}{60}\right)^2)$	-
V Shape with gaps [66]	$Nu = 0.000018\ Re^{0.9635} N_g^{0.126} \left(\frac{g}{e}\right)^{0.111} \left(\frac{\alpha}{60}\right)^{0.1307} \left(\frac{P}{e}\right)^{5.7419} \times \exp\left(-0.555 * \left(\ln N_g\right)^2\right) * \exp\left[-0.04011 \left(\ln\left(\frac{g}{e}\right)\right)^2\right] \times \exp\left[-1.299 \left(\ln\left(\frac{P}{e}\right)\right)^2\right] \times \exp\left[-0.04011 \left(\ln\left(\frac{\alpha}{60}\right)\right)^2\right]$	η_{th}=75% η_{eff}=68%

	$f = 0.0000036\,Re^{-0.1521}N_g^{0.184}\left(\frac{g}{e}\right)^{0.072}\left(\frac{\alpha}{60}\right)^{0.07}\left(\frac{P}{e}\right)^{9.24} \times \exp(-0.0763 * (\ln N_g)^2) * \exp\left[-0.0249\left(\ln\left(\frac{g}{e}\right)\right)^2\right] \times \exp\left[-2.08\left(\ln\left(\frac{P}{e}\right)\right)^2\right] \times \exp\left[-0.3364\left(\ln\left(\frac{\alpha}{60}\right)\right)^2\right]$	
Discrete Multi V [104]	$Nu = 0.008532\,Re^{0.9635}\left(\frac{e}{D}\right)^{0.175}\left(\frac{W}{w}\right)^{0.506}\left(\frac{Gd}{Lv}\right)^{-0.0348}\left(\frac{\alpha}{60}\right)^{-0.0239}\left(\frac{g}{e}\right)^{-0.0708}($ $\times \exp\left[-0.223\left(\ln\left(\frac{g}{e}\right)\right)^2\right] \times \exp\left[-0.0753\left(\ln\left(\frac{W}{w}\right)\right)^2\right]$ $\times \exp\left[-0.0653\left(\ln\left(\frac{Gd}{Lv}\right)\right)^2\right] \times \exp\left[0.1153\left(\ln\left(\frac{\alpha}{60}\right)\right)^2\right] \times$ $\times \exp\left[-0.285\left(\ln\left(\frac{P}{e}\right)\right)^2\right]$ $f = 3.94\,Re^{-0.3151}\left(\frac{e}{D}\right)^{.268}\left(\frac{W}{w}\right)^{0.1132}\left(\frac{Gd}{Lv}\right)^{0.610}\left(\frac{\alpha}{60}\right)^{0.1553}\left(\frac{g}{e}\right)^{-0.1769}\left(\frac{P}{e}\right)^{-0.79}$ $\times \exp\left[-0.6349\left(\ln\left(\frac{g}{e}\right)\right)^2\right] \times \exp\left[0.0974\left(\ln\left(\frac{W}{w}\right)\right)^2\right]$ $\times \exp\left[-0.1065\left(\ln\left(\frac{Gd}{Lv}\right)\right)^2\right] \times \exp\left[-0.1527\left(\ln\left(\frac{\alpha}{60}\right)\right)^2\right] \times$ $\times \exp\left[0.1486\left(\ln\left(\frac{P}{e}\right)\right)^2\right]$	η_{eff}=62.4%
Arc [105]	$Nu = 0.001047\,Re^{1.3186}\left(\frac{e}{D}\right)^{0.3772}\left(\frac{\alpha}{90}\right)^{-0.1198}$ $f = 0.14408\,Re^{-0.17103}\left(\frac{e}{D}\right)^{0.1765}\left(\frac{\alpha}{90}\right)^{0.1185}$	η_{th}=79.84 % η_{eff}=75.24 %
S Shape[63]	$Nu = 0.00014332\,Re^{1.274}\left(\frac{e}{D_h}\right)^{-0.7653}\left(\frac{W}{w}\right)^{0.2748}\left(\frac{\alpha}{90}\right)^{0.1553}\left(\frac{P}{e}\right)^{0.4876}$ $\times \exp\left[-0.1084\left(\ln\left(\frac{W}{w}\right)\right)^2\right] \times \exp\left[-0.1257\left(\ln\left(\frac{e}{D_h}\right)\right)^2\right]$ $\times\times \exp\left[-0.1107\left(\ln\left(\frac{P}{e}\right)\right)^2\right] \times \exp\left[-0.642\left(\ln\left(\frac{\alpha}{90}\right)\right)^2\right]$ $f = 0.143\,Re^{-0.224}\left(\frac{e}{D_h}\right)^{0.2159}\left(\frac{W}{w}\right)^{0.1424}\left(\frac{\alpha}{90}\right)^{0.1553}\left(\frac{g}{e}\right)^{0.2129}\left(\frac{P}{e}\right)^{0.7657} \times$ $\times \exp\left[-0.187\left(\ln\left(\frac{P}{e}\right)\right)^2\right]$	-
Baffle shape	**Correlations**	**Major Findings**

Ribs and baffles [62]	$\eta_{eff} = 0.00000676\,Re^{3.4221}\left(\frac{L_B}{L}\right)^{0.1328}\left(\frac{W_B}{W}\right)^{-0.3316} \times (N_0)^{0.1137} \times \exp\left[-0.1933(\ln(Re))^2\right] \times \exp\left[-0o254\left(\ln\left(\frac{W_B}{W}\right)\right)^2\right] \times \times \exp\left[0.05\left(\ln\left(\frac{L_B}{L}\right)\right)^2\right] \times \exp\left[-0.0242(\ln(N_0))^2\right]$	η_{th}=81.9% η_{eff}=28%
Wave like baffles [93]	-	η_{th}=75%
Rectangular and V baffles[106]		η_{th}=27% greater than no baffle case

4. CONCLUSION

In the present work, a comprehensive evaluation on the performance enhancing strategies of solar air heaters are offered. Numerous active and passive strategies have been documented by researchers to increase the performance of SAHs using numerical and experimental study. The passive techniques have been accepted largely because of convenience in the installation and utilization. Providing ribs and baffles beneath the heat-absorbing surface of SAH are the best passive approaches documented in the broad literature. The height of ribs have remained suitably high so the viscous laminar layer can break apart. The heat transmission has discovered increased by inserting ribs of nominal height on the surface due of turbulence caused by ribs. However, the friction factor also increased but overall performance of SAH also enhanced. To further boost the heat transfer, researchers have inserted several ribs on the surface i.e. increased the number of ribs. The boost in the number ribs had shown to be an excellent idea as the rate of heat transfer increased. The instant significant of putting many ribs has also resulted in the amplification of friction factor. The investigations have been further extended to find the thermal, effective and exergy efficiencies of SAH with thermo-hydraulic performance. The rationale for estimating these efficiencies is that the quantity of the heat loss, beneficial heat gain and matching friction losses. To compute thermal and effective efficiency, the researchers have employed correlations. These correlations have been feed into the numerical codes and the ideal set of parameters within the whole range of researched parameters in that particular study. The exergy losses have also been computed and discussed among numerous studies.

In the equivalent pursuit, researchers have employed baffles for the heat transfer augmentations. The usage of baffles has considerably boosted the heat transmission because the turbulence created by baffles. However, the friction factor has increased several folds too. Nevertheless, the thermo-hydraulic performance was been increased in comparison to the ribs. The thermal efficiency has also increased, but effective efficiency has dropped due to increasing friction losses. To alleviate the worries of increasing friction factor, the perforated baffles have been adopted. The perforation in the baffles has minimized the friction factor and boosted the effective efficiency. The researchers have also used gaps in baffles, combination of ribs and baffles, putting baffles in staggered manner in such a way that to encourage the reattachment zones.

REFERENCES

[1] R. Kumar, A. Kumar, and V. Goel, 'A parametric analysis of rectangular rib roughened triangular duct solar air heater using computational fluid dynamics', Solar Energy, vol. 157, no. February, pp. 1095–1107, 2017, doi: 10.1016/j.solener.2017.08.071.
[2] K. Nidhul, S. Kumar, A. K. Yadav, and S. Anish, 'Enhanced thermo-hydraulic performance in a V-ribbed triangular duct solar air heater: CFD and exergy analysis', Energy, vol. 200, p. 117448, 2020, doi: 10.1016/j.energy.2020.117448.
[3] H. F. Oztop, F. Bayrak, and A. Hepbasli, 'Energetic and exergetic aspects of solar air heating (solar collector) systems', Renewable and Sustainable Energy Reviews, vol. 21, pp. 59–83, 2013, doi: 10.1016/j.rser.2012.12.019.
[4] B. Madhu et al., 'Investigation on heat transfer enhancement of conventional and staggered fin solar air heater coated with CNT-black paint—an experimental approach', Environmental Science and Pollution Research, 2020, doi: 10.1007/s11356-019-07561-1.

[5] T. K. Abdelkader, Y. Zhang, E. S. Gaballah, S. Wang, Q. Wan, and Q. Fan, 'Energy and exergy analysis of a flat-plate solar air heater coated with carbon nanotubes and cupric oxide nanoparticles embedded in black paint', Journal of Cleaner Production, vol. 250, no. May 2020, 2020, doi: 10.1016/j.jclepro.2019.119501.
[6] G. Tanda, 'Performance of solar air heater ducts with different types of ribs on the absorber plate', Energy, vol. 36, no. 11, pp. 6651–6660, Nov. 2011, doi: 10.1016/J.ENERGY.2011.08.043.
[7] K. D. Yadav and R. K. Prasad, 'Performance analysis of parallel flow flat plate solar air heater having arc shaped wire roughened absorber plate', Renewable Energy Focus, vol. 32, pp. 23–44, 2020, doi: https://doi.org/10.1016/j.ref.2019.10.002.
[8] D. Wang, J. Liu, Y. Liu, Y. Wang, B. Li, and J. Liu, 'Evaluation of the performance of an improved solar air heater with "S" shaped ribs with gap', Solar Energy, vol. 195, pp. 89–101, 2020, doi: https://doi.org/10.1016/j.solener.2019.11.034.
[9] A. Kumar, R. P. Saini, and J. S. Saini, 'Development of correlations for Nusselt number and friction factor for solar air heater with roughened duct having multi v-shaped with gap rib as artificial roughness', Renewable Energy, vol. 58, pp. 151–163, 2013, doi: https://doi.org/10.1016/j.renene.2013.03.013.
[10]S. [Singh Patel and A. Lanjewar, 'Experimental and numerical investigation of solar air heater with novel V-rib geometry', Journal of Energy Storage, vol. 21, pp. 750–764, 2019, doi: https://doi.org/10.1016/j.est.2019.01.016.
[11]G. K. Poongavanam, K. Panchabikesan, A. J. D. Leo, and V. Ramalingam, 'Experimental investigation on heat transfer augmentation of solar air heater using shot blasted V-corrugated absorber plate', Renewable Energy, vol. 127, pp. 213–229, 2018, doi: https://doi.org/10.1016/j.renene.2018.04.056.
[12]A. Kumar and A. Layek, 'Energetic and exergetic performance evaluation of solar air heater with twisted rib roughness on absorber plate', Journal of Cleaner Production, vol. 232, pp. 617–628, 2019, doi: https://doi.org/10.1016/j.jclepro.2019.05.363.
[13]M. K. Sahu and R. K. Prasad, 'Exergy based performance evaluation of solar air heater with arc-shaped wire roughened absorber plate', Renewable Energy, vol. 96, pp. 233–243, 2016, doi: https://doi.org/10.1016/j.renene.2016.04.083.
[14]I. Singh, S. Vardhan, S. Singh, and A. Singh, 'Experimental and CFD analysis of solar air heater duct roughened with multiple broken transverse ribs: A comparative study', Solar Energy, vol. 188, pp. 519–532, 2019, doi: https://doi.org/10.1016/j.solener.2019.06.022.
[15]V. B. Gawande, A. S. Dhoble, D. B. Zodpe, and S. Chamoli, 'Experimental and CFD investigation of convection heat transfer in solar air heater with reverse L-shaped ribs', Solar Energy, vol. 131, pp. 275–295, 2016, doi: https://doi.org/10.1016/j.solener.2016.02.040.
[16]R. Kumar, S. Kumar Verma, and V. Kumar Sharma, 'Performance enhancement analysis of triangular solar air heater coated with nanomaterial embedded in black paint', Materials Today: Proceedings, Mar. 2020, doi: 10.1016/j.matpr.2020.02.538.
[17]M. S. Manjunath, K. V. Karanth, and N. Y. Sharma, 'Numerical analysis of the influence of spherical turbulence generators on heat transfer enhancement of flat plate solar air heater', Energy, vol. 121, pp. 616–630, 2017, doi: https://doi.org/10.1016/j.energy.2017.01.032.
[18]Y. Varol, H. F. Oztop, and T. Yilmaz, 'Natural convection in triangular enclosures with protruding isothermal heater', International Journal of Heat and Mass Transfer, vol. 50, no. 13–14, pp. 2451–2462, 2007, doi: 10.1016/j.ijheatmasstransfer.2006.12.027.
[19]A. S. Yadav and J. L. Bhagoria, 'A CFD analysis of a solar air heater having triangular rib roughness on the absorber plate', International Journal of ChemTech Research, vol. 5, no. 2, pp. 964–971, 2013.
[20]S. Skullong, S. Kwankaomeng, C. Thianpong, and P. Promvonge, 'Thermal performance of turbulent fl ow in a solar air heater channel with', International Communications in Heat and Mass Transfer, vol. 50, pp. 34–43, 2014, doi: 10.1016/j.icheatmasstransfer.2013.11.001.
[21]B. Bhushan and R. Singh, 'A review on methodology of artificial roughness used in duct of solar air heaters', Energy, vol. 35, no. 1, pp. 202–212, Jan. 2010, doi: 10.1016/J.ENERGY.2009.09.010.
[22]T. Zhu, Y. Diao, Y. Zhao, and C. Ma, 'Performance evaluation of a novel flat-plate solar air collector with micro-heat pipe arrays (MHPA)', Applied Thermal Engineering, vol. 118, pp. 1–16, 2017, doi: 10.1016/j.applthermaleng.2017.02.076.
[23]S. K. Mishra, R. Kumar, R. Joshi, H. Kumar, and N. Saxena, 'Experimental Investigation, Exergy Analysis, and CFD Simulation of Solar Air Heater Roughened with Artificial V-Shaped Ribs on Absorber Surface Artificial Roughness on Absorber Plate', pp. 235–252, 2021, doi: 10.1007/978-981-16-0235-1_20.
[24]R. Kumar, A. Kumar, and V. Goel, 'Performance improvement and development of correlation for friction factor and heat transfer using computational fluid dynamics for ribbed triangular duct solar air heater', Renewable Energy, vol. 131, pp. 788–799, 2019, doi: 10.1016/j.renene.2018.07.078.
[25]A. Kumar and A. Layek, 'Energetic and exergetic performance evaluation of solar air heater with twisted rib roughness on absorber plate', Journal of Cleaner Production, vol. 232, pp. 617–628, 2019, doi: 10.1016/j.jclepro.2019.05.363.
[26]S. Singh, 'Experimental and numerical investigations of a single and double pass porous serpentine wavy wiremesh packed bed solar air heater', Renewable Energy, vol. 145, pp. 1361–1387, Jan. 2020, doi: 10.1016/J.RENENE.2019.06.137.
[27]S. Singh, 'Thermal performance analysis of semicircular and triangular cross-sectioned duct solar air heaters under external recycle', Journal of Energy Storage, vol. 20, no. October, pp. 316–336, 2018, doi: 10.1016/j.est.2018.10.003.
[28]R. P. Saini and J. Verma, 'Heat transfer and friction factor correlations for a duct having dimple-shape artificial roughness for solar air heaters', Energy, vol. 33, no. 8, pp. 1277–1287, Aug. 2008, doi: 10.1016/J.ENERGY.2008.02.017.
[29]A. Lanjewar, J. L. Bhagoria, and R. M. Sarviya, 'Experimental study of augmented heat transfer and friction in solar air heater with different orientations of W-Rib roughness', Experimental Thermal and Fluid Science, vol. 35, no. 6, pp. 986–995, Sep. 2011, doi: 10.1016/J.EXPTHERMFLUSCI.2011.01.019.
[30]M. A. Karim and M. N. A. Hawlader, 'Performance investigation of flat plate, v-corrugated and finned air collectors', Energy, vol. 31, no. 4, pp. 452–470, Mar. 2006, doi: 10.1016/J.ENERGY.2005.03.007.
[31]A. Priyam and P. Chand, 'Thermal and thermohydraulic performance of wavy finned absorber solar air heater', Solar Energy, vol. 130, pp. 250–259, Jun. 2016, doi: 10.1016/J.SOLENER.2016.02.030.

[32]R. S. Gill, V. S. Hans, and S. Singh, 'Investigations on thermo-hydraulic performance of broken arc rib in a rectangular duct of solar air heater', International Communications in Heat and Mass Transfer, vol. 88, pp. 20–27, 2017, doi: 10.1016/j.icheatmasstransfer.2017.07.024.
[33]'Design analysis of corrugated and flat plate solar air heaters'. http://eprint.iitd.ac.in/handle/2074/2538 (accessed Apr. 20, 2022).
[34]M. E. Taslim, T. Li, and D. M. Kercher, 'Experimental Heat Transfer and Friction in Channels Roughened With Angled, V-Shaped and Discrete Ribs on Two Opposite Walls', American Society of Mechanical Engineers (Paper), pp. 1–11, Feb. 2015, doi: 10.1115/94-GT-163.
[35]H. K. Ghritlahre and R. K. Prasad, 'Exergetic performance prediction of solar air heater using MLP, GRNN and RBF models of artificial neural network technique', Journal of Environmental Management, vol. 223, pp. 566–575, Oct. 2018, doi: 10.1016/J.JENVMAN.2018.06.033.
[36]K. Nidhul, A. K. Yadav, S. Anish, and S. Kumar, 'Critical review of ribbed solar air heater and performance evaluation of various V-rib configuration', Renewable and Sustainable Energy Reviews, vol. 142, no. May 2020, p. 110871, 2021, doi: 10.1016/j.rser.2021.110871.
[37]V. Singh Bisht, A. Kumar Patil, and A. Gupta, 'Review and performance evaluation of roughened solar air heaters', Renewable and Sustainable Energy Reviews, vol. 81, no. May 2017, pp. 954–977, 2018, doi: 10.1016/j.rser.2017.08.036.
[38]S. K. Sharma and V. R. Kalamkar, 'Experimental and numerical investigation of forced convective heat transfer in solar air heater with thin ribs', Solar Energy, vol. 147, pp. 277–291, 2017, doi: 10.1016/j.solener.2017.03.042.
[39]F. Chabane, F. Grira, N. Moummi, and A. Brima, 'Experimental study of a solar air heater by adding an arrangement of transverse rectangular baffles perpendicular to the air stream', International Journal of Green Energy, vol. 16, no. 14, pp. 1264–1277, 2019, doi: 10.1080/15435075.2019.1671401.
[40]A. Z. Aghaie, A. B. Rahimi, and A. Akbarzadeh, 'A general optimized geometry of angled ribs for enhancing the thermo-hydraulic behavior of a solar air heater channel e A Taguchi approach', Renewable Energy, vol. 83, pp. 47–54, 2015, doi: 10.1016/j.renene.2015.04.016.
[41]A. Kumar and M.-H. Kim, 'Thermal Hydraulic Performance in a Solar Air Heater Channel with Multi V-Type Perforated Baffles', Energies, vol. 9, no. 7. p. 564, 2016. doi: 10.3390/en9070564.
[42]D. Jin, S. Quan, J. Zuo, and S. Xu, 'Numerical investigation of heat transfer enhancement in a solar air heater roughened by multiple V-shaped ribs', Renewable Energy, 2019, doi: 10.1016/j.renene.2018.11.016.
[43]S. Sharma, R. K. Das, and K. Kulkarni, 'Performance Evaluation of Solar Air Heater Using Sine Wave Shape Obstacle', in Current Advances in Mechanical Engineering, 2021, pp. 541–553.
[44]S. K. Jain, G. Das Agrawal, and R. Misra, 'Experimental Investigation of Thermohydraulic Performance of the Solar Air Heater Having Arc- Shaped Ribs With Multiple Gaps', vol. 12, no. February, pp. 1–10, 2020, doi: 10.1115/1.4044427.
[45]P. T. Saravanakumar, D. Somasundaram, and M. M. Matheswaran, 'Exergetic investigation and optimization of arc shaped rib roughened solar air heater integrated with fins and baffles', Applied Thermal Engineering, vol. 175, no. March, p. 115316, 2020, doi: 10.1016/j.applthermaleng.2020.115316.
[46]Y. M. Patel, S. V Jain, and V. J. Lakhera, 'Thermo-hydraulic performance analysis of a solar air heater roughened with reverse NACA profile ribs National Advisory Committee for Aeronautics', Applied Thermal Engineering, vol. 170, no. September 2019, p. 114940, 2020, doi: 10.1016/j.applthermaleng.2020.114940.
[47]B. Sahin, I. Ates, E. Manay, A. Bayrakceken, and C. Celik, 'Optimization of design parameters for heat transfer and friction factor in a heat sink with hollow trapezoidal baffles', Applied Thermal Engineering, vol. 154, no. January, pp. 76–86, 2019, doi: 10.1016/j.applthermaleng.2019.03.056.
[48]K. Prasad and S. C. Mullick, 'Heat transfer characteristics of a solar air heater used for drying purposes', Applied Energy, vol. 13, no. 2, pp. 83–93, 1983, doi: 10.1016/0306-2619(83)90001-6.
[49]B. N. Prasad and J. S. Saini, 'Effect of artificial roughness on heat transfer and friction factor in a solar air heater', Solar Energy, vol. 41, no. 6, pp. 555–560, 1988, doi: https://doi.org/10.1016/0038-092X(88)90058-8.
[50]D. Gupta, S. C. Solanki, and J. S. Saini, 'Heat and fluid flow in rectangular solar air heater ducts having transverse rib roughness on absorber plates', Solar Energy, vol. 51, no. 1, pp. 31–37, Jul. 1993, doi: 10.1016/0038-092X(93)90039-Q.
[51]M. M. Sahu and J. L. Bhagoria, 'Augmentation of heat transfer coefficient by using 90° broken transverse ribs on absorber plate of solar air heater', Renewable Energy, vol. 30, no. 13, pp. 2057–2073, 2005, doi: 10.1016/j.renene.2004.10.016.
[52]Y. Ho-Ming and C. Wen-Hsen, 'Efficiency of solar air heaters with baffles', Energy, vol. 16, no. 7, pp. 983–987, 1991, doi: 10.1016/0360-5442(91)90058-T.
[53]R. A. Damseh, 'Pergamon SOLAR AIR HEATERS Abstract–A', vol. 13, no. 2, pp. 153–163, 1998.
[54]D. Gupta, S. C. Solanki, and J. S. Saini, 'Thermohydraulic performance of solar air heaters with roughened absorber plates', Solar Energy, vol. 61, no. 1, pp. 33–42, 1997, doi: https://doi.org/10.1016/S0038-092X(97)00005-4.
[55]K. R. Aharwal, B. K. Gandhi, and J. S. Saini, 'Experimental investigation on heat-transfer enhancement due to a gap in an inclined continuous rib arrangement in a rectangular duct of solar air heater', vol. 33, pp. 585–596, 2008, doi: 10.1016/j.renene.2007.03.023.
[56]K. R. Aharwal, B. K. Gandhi, and J. S. Saini, 'International Journal of Heat and Mass Transfer Heat transfer and friction characteristics of solar air heater ducts having integral inclined discrete ribs on absorber plate', International Journal of Heat and Mass Transfer, vol. 52, no. 25–26, pp. 5970–5977, 2009, doi: 10.1016/j.ijheatmasstransfer.2009.05.032.
[57]P. Dutta and A. Hossain, 'Internal cooling augmentation in rectangular channel using two inclined baffles', vol. 26, pp. 223–232, 2005, doi: 10.1016/j.ijheatfluidflow.2004.08.001.
[58]P. Promvonge, S. Sripattanapipat, S. Tamna, S. Kwankaomeng, and C. Thianpong, 'Numerical investigation of laminar heat transfer in a square channel with 45 ° inclined baf fl es ☆', International Communications in Heat and Mass Transfer, vol. 37, no. 2, pp. 170–177, 2010, doi: 10.1016/j.icheatmasstransfer.2009.09.010.

[59]A. P. Singh, Varun, and Siddhartha, 'Effect of artificial roughness on heat transfer and friction characteristics having multiple arc shaped roughness element on the absorber plate', Solar Energy, vol. 105, pp. 479–493, 2014, doi: 10.1016/j.solener.2014.04.007.
[60]N. K. Pandey and V. K. Bajpai, 'Experimental investigation of heat transfer augmentation using multiple arcs with gap on absorber plate of solar air heater', Solar Energy, vol. 134, pp. 314–326, 2016, doi: 10.1016/j.solener.2016.05.007.
[61]N. Koolnapadol, Y. Kaewkohkiat, and P. Promvonge, 'Thermal Behaviors in a Solar Air Heater Channel with Arc-Shaped Baffle Turbulators', vol. 1051, pp. 845–849, 2014, doi: 10.4028/www.scientific.net/AMR.1051.845.
[62]P. T. Saravanakumar, D. Somasundaram, and M. M. Matheswaran, 'Thermal and thermo-hydraulic analysis of arc shaped rib roughened solar air heater integrated with fins and baffles', Solar Energy, vol. 180, no. October 2018, pp. 360–371, 2019, doi: 10.1016/j.solener.2019.01.036.
[63]K. Kumar, D. R. Prajapati, and S. Samir, 'Heat transfer and friction factor correlations development for solar air heater duct artificially roughened with " S " shape ribs', Experimental Thermal and Fluid Science, vol. 82, pp. 249–261, 2017, doi: 10.1016/j.expthermflusci.2016.11.012.
[64]D. Wang, J. Liu, Y. Liu, Y. Wang, B. Li, and J. Liu, 'Evaluation of the performance of an improved solar air heater with "S" shaped ribs with gap', Solar Energy, vol. 195, no. 13, pp. 89–101, 2020, doi: 10.1016/j.solener.2019.11.034.
[65]J. C. Han, Y. M. Zhang, and C. P. Lee, 'Augmented heat transfer in square channels with parallel, crossed, and v-shaped angled ribs', Journal of Heat Transfer, vol. 113, no. 3, pp. 590–596, 1991, doi: 10.1115/1.2910606.
[66]R. Maithani and J. S. Saini, 'Performance evaluation of solar air heater having V-ribs with symmetrical gaps in a rectangular duct of solar air heater', vol. 0750, no. October, 2017, doi: 10.1080/01430750.2015.1133455.
[67]D. Jin, J. Zuo, S. Quan, S. Xu, and H. Gao, 'Thermohydraulic performance of solar air heater with staggered multiple V-shaped ribs on the absorber plate', Energy, vol. 127, pp. 68–77, 2017, doi: 10.1016/j.energy.2017.03.101.
[68]'single perforated.pdf'.
[69]S. K. Jain, R. Misra, A. Kumar, and G. Das Agrawal, 'Thermal performance investigation of a solar air heater having discrete V-shaped perforated baffles', International Journal of Ambient Energy, vol. 0, no. 0, pp. 1–9, 2019, doi: 10.1080/01430750.2019.1636874.
[70]R. Kumar, A. Kumar, A. Sharma, R. Chauhan, and M. Sethi, 'Experimental study of heat transfer enhancement in a rectangular duct distributed by multi V-perforated baffle of different relative baffle width', Heat and Mass Transfer/Waerme-und Stoffuebertragung, vol. 53, no. 4, pp. 1289–1304, 2017, doi: 10.1007/s00231-016-1901-7.
[71]R. P. Ã. Saini and J. Verma, 'Heat transfer and friction factor correlations for a duct having dimple-shape artificial roughness for solar air heaters', vol. 33, pp. 1277–1287, 2008, doi: 10.1016/j.energy.2008.02.017.
[72]V. B. Gawande, A. S. Dhoble, D. B. Zodpe, and S. Chamoli, 'ScienceDirect Experimental and CFD investigation of convection heat transfer in solar air heater with reverse L-shaped ribs', Solar Energy, vol. 131, pp. 275–295, 2016, doi: 10.1016/j.solener.2016.02.040.
[73]J. S. Saini, 'Heat transfer and friction factor correlations for artificially roughened ducts with expanded metal mesh as roughness element', 1996.
[74]S. V Karmare and A. N. Tikekar, 'Heat transfer and friction factor correlation for artificially roughened duct with metal grit ribs', vol. 50, pp. 4342–4351, 2007, doi: 10.1016/j.ijheatmasstransfer.2007.01.065.
[75]A. Kumar and A. Layek, 'Nusselt number and friction factor correlation of solar air heater having twisted-rib roughness on absorber plate', Renewable Energy, vol. 130, pp. 687–699, 2019, doi: 10.1016/j.renene.2018.06.076.
[76]S. B. Bopche and M. S. Tandale, 'International Journal of Heat and Mass Transfer Experimental investigations on heat transfer and frictional characteristics of a turbulator roughened solar air heater duct', International Journal of Heat and Mass Transfer, vol. 52, no. 11–12, pp. 2834–2848, 2009, doi: 10.1016/j.ijheatmasstransfer.2008.09.039.
[77]A. Kumar, J. L. Bhagoria, and R. M. Sarviya, 'Heat transfer and friction correlations for artificially roughened solar air heater duct with discrete W-shaped ribs', Energy Conversion and Management, vol. 50, no. 8, pp. 2106–2117, 2009, doi: 10.1016/j.enconman.2009.01.025.
[78]A. Lanjewar, J. L. Bhagoria, and R. M. Sarviya, 'Experimental study of augmented heat transfer and friction in solar air heater with different orientations of W-Rib roughness', Experimental Thermal and Fluid Science, vol. 35, no. 6, pp. 986–995, 2011, doi: 10.1016/j.expthermflusci.2011.01.019.
[79]E. M. S. El-said, 'Numerical investigations of fluid flow and heat transfer characteristics in solar air collector with curved perforated baffles', no. January, pp. 1–15, 2020, doi: 10.1002/eng2.12142.
[80]A. Khanlari et al., 'Experimental and numerical study of the effect of integrating plus-shaped perforated baffles to solar air collector in drying application', Renewable Energy, vol. 145, pp. 1677–1692, 2020, doi: 10.1016/j.renene.2019.07.076.
[81]J. J. Fiuk and K. Dutkowski, 'Experimental investigations on thermal e ffi ciency of a prototype passive solar air collector with wavelike ba ffl es', Solar Energy, vol. 188, no. March, pp. 495–506, 2019, doi: 10.1016/j.solener.2019.06.030.
[82]P. Sriromreun, C. Thianpong, and P. Promvonge, 'Experimental and numerical study on heat transfer enhancement in a channel with Z-shaped baf fl es ☆', International Communications in Heat and Mass Transfer, vol. 39, no. 7, pp. 945–952, 2012, doi: 10.1016/j.icheatmasstransfer.2012.05.016.
[83]R. Nadda, R. Maithani, and A. Kumar, 'Effect of multiple arc protrusion ribs on heat transfer and fluid flow of a circular-jet impingement solar air passage', Chemical Engineering and Processing: Process Intensification, vol. 120, no. July, pp. 114–133, 2017, doi: 10.1016/j.cep.2017.07.005.
[84]R. Kant and R. P. Saini, 'A review on different techniques used for performance enhancement of double pass solar air heaters', Renewable and Sustainable Energy Reviews, vol. 56, pp. 941–952, 2016, doi: 10.1016/j.rser.2015.12.004.
[85]A. E. Kabeel, M. H. Hamed, Z. M. Omara, and A. W. Kandeal, 'Solar air heaters : Design con fi gurations , improvement methods and applications – A detailed review', vol. 70, no. November 2015, pp. 1189–1206, 2017, doi: 10.1016/j.rser.2016.12.021.

[86]A. Saxena and A. A. El-sebaii, 'A thermodynamic review of solar air heaters', Renewable and Sustainable Energy Reviews, vol. 43, pp. 863–890, 2015, doi: 10.1016/j.rser.2014.11.059.
[87]A. K. Babu, G. Kumaresan, V. A. A. Raj, and R. Velraj, 'Review of leaf drying: Mechanism and influencing parameters, drying methods, nutrient preservation, and mathematical models', Renewable and Sustainable Energy Reviews, vol. 90, no. December 2016, pp. 536–556, 2018, doi: 10.1016/j.rser.2018.04.002.
[88]V. B. Gawande, A. S. Dhoble, D. B. Zodpe, and S. Chamoli, 'A review of CFD methodology used in literature for predicting thermo-hydraulic performance of a roughened solar air heater', Renewable and Sustainable Energy Reviews, vol. 54, pp. 550–605, 2016, doi: 10.1016/j.rser.2015.10.025.
[89]R. Kumar, V. Goel, and A. Kumar, 'Investigation of heat transfer augmentation and friction factor in triangular duct solar air heater due to forward facing chamfered rectangular ribs: A CFD based analysis', Renewable Energy, vol. 115, pp. 824–835, 2018, doi: 10.1016/j.renene.2017.09.010.
[90]I. Singh and S. Singh, 'CFD analysis of solar air heater duct having square wave pro fi led transverse ribs as roughness elements', Solar Energy, vol. 162, no. July 2017, pp. 442–453, 2018, doi: 10.1016/j.solener.2018.01.019.
[91]'Thermo-hydraulic performance analysis of a solar air heater (SAH) with quarter-circular ribs on the absorber plate_ A comparative study _ Enhanced Reader.pdf'.
[92]A. S. Yadav and J. L. Bhagoria, 'A CFD based thermo-hydraulic performance analysis of an artificially roughened solar air heater having equilateral triangular sectioned rib roughness on the absorber plate', International Journal of Heat and Mass Transfer, vol. 70, pp. 1016–1039, 2014, doi: https://doi.org/10.1016/j.ijheatmasstransfer.2013.11.074.
[93]J. J. Fiuk and K. Dutkowski, 'Experimental investigations on thermal e ffi ciency of a prototype passive solar air collector with wavelike ba ffl es', Solar Energy, vol. 188, no. March, pp. 495–506, 2019, doi: 10.1016/j.solener.2019.06.030.
[94]R. Nadda, A. Kumar, and R. Maithani, 'Developing heat transfer and friction loss in an impingement jets solar air heater with multiple arc protrusion obstacles', Solar Energy, vol. 158, no. October, pp. 117–131, 2017, doi: 10.1016/j.solener.2017.09.042.
[95]A. Priyam and P. Chand, 'Effect of wavelength and amplitude on the performance of wavy fi nned absorber solar air heater', Renewable Energy, vol. 119, pp. 690–702, 2018, doi: 10.1016/j.renene.2017.12.010.
[96]H. Hassan, S. Abo-elfadl, and M. F. El-dosoky, 'An experimental investigation of the performance of new design of solar air heater (tubular)', Renewable Energy, vol. 151, pp. 1055–1066, 2020, doi: 10.1016/j.renene.2019.11.112.
[97]A. K. Goel, S. N. Singh, and B. N. Prasad, 'Performance investigation and parametric optimization of an eco-friendly sustainable design solar air heater', no. March, pp. 1–12, 2021, doi: 10.1049/rpg2.12188.
[98]A. Kumar and A. Layek, 'Energetic and exergetic performance evaluation of solar air heater with twisted rib roughness on absorber plate', Journal of Cleaner Production, vol. 232, pp. 617–628, 2019, doi: 10.1016/j.jclepro.2019.05.363.
[99]A. K. Raj, M. Srinivas, and S. Jayaraj, 'A cost-e ff ective method to improve the performance of solar air heaters using discrete macro-encapsulated PCM capsules for drying applications', Applied Thermal Engineering, vol. 146, no. October 2018, pp. 910–920, 2019, doi: 10.1016/j.applthermaleng.2018.10.055.
[100]P. T. Saravanakumar, D. Somasundaram, and M. M. Matheswaran, 'Exergetic investigation and optimization of arc shaped rib roughened solar air heater integrated with fins and baffles', Applied Thermal Engineering, vol. 175, no. April, p. 115316, 2020, doi: 10.1016/j.applthermaleng.2020.115316.
[101]R. Kumar and P. Chand, 'Performance enhancement of solar air heater using herringbone corrugated fi ns', Energy, vol. 127, pp. 271–279, 2017, doi: 10.1016/j.energy.2017.03.128.
[102]V. B. Gawande, A. S. Dhoble, D. B. Zodpe, and S. Chamoli, 'Analytical approach for evaluation of thermo hydraulic performance of roughened solar air heater', Case Studies in Thermal Engineering, vol. 8, pp. 19–31, 2016, doi: 10.1016/j.csite.2016.03.003.
[103]A.-M. Ebrahim Momin, J. S. Saini, and S. C. Solanki, 'Heat transfer and friction in solar air heater duct with V-shaped rib roughness on absorber plate', International Journal of Heat and Mass Transfer, vol. 45, no. 16, pp. 3383–3396, 2002, doi: https://doi.org/10.1016/S0017-9310(02)00046-7.
[104]A. Kumar, R. P. Saini, and J. S. Saini, 'Numerical simulation of effective efficiency of a discrete multi V-pattern rib solar air channel', Heat and Mass Transfer, doi: 10.1007/s00231-015-1712-2.
[105]M. K. Sahu and R. K. Prasad, 'Thermohydraulic performance analysis of an arc shape wire roughened solar air heater', Renewable Energy, vol. 108, pp. 598–614, 2017, doi: 10.1016/j.renene.2017.02.075.
[106]H. Olfian, A. Zabihi Sheshpoli, and S. S. Mousavi Ajarostaghi, 'Numerical evaluation of the thermal performance of a solar air heater equipped with two different types of baffles', Heat Transfer - Asian Research, no. December, pp. 1–21, 2020, doi: 10.1002/htj.21656.